



HAL
open science

Hygrothermal performance of multilayer straw walls in different climates

Ghadie Tlaji, Fabienne Pennec, Salah Ouldboukhitine, Mohamad Ibrahim, Pascal Henry Biwolé

► **To cite this version:**

Ghadie Tlaji, Fabienne Pennec, Salah Ouldboukhitine, Mohamad Ibrahim, Pascal Henry Biwolé. Hygrothermal performance of multilayer straw walls in different climates. *Construction and Building Materials*, 2022, 326, pp.126873. 10.1016/j.conbuildmat.2022.126873 . hal-03590913

HAL Id: hal-03590913

<https://uca.hal.science/hal-03590913>

Submitted on 22 Jul 2024

HAL is a multi-disciplinary open access archive for the deposit and dissemination of scientific research documents, whether they are published or not. The documents may come from teaching and research institutions in France or abroad, or from public or private research centers.

L'archive ouverte pluridisciplinaire **HAL**, est destinée au dépôt et à la diffusion de documents scientifiques de niveau recherche, publiés ou non, émanant des établissements d'enseignement et de recherche français ou étrangers, des laboratoires publics ou privés.



Distributed under a Creative Commons Attribution - NonCommercial 4.0 International License

Hygrothermal Performance of Multilayer Straw Walls in Different Climates

Ghadie Tlaji^a, Fabienne Pennec^a, Salah Ouldboukhitine^a, Mohamad Ibrahim^c, Pascal Biwole^{a, b*}

^(a) Université Clermont Auvergne, CNRS, Clermont Auvergne INP, Institut Pascal, F-63000 Clermont–Ferrand, France

^(b) MINES Paris Tech, PSL Research University, PERSEE - Center for Processes, Renewable Energies and Energy Systems, CS 10207, 06 904 Sophia Antipolis, France

^(c) Polytech'Lab, UPR UCA 7498, Université Cote d'Azur, 930 Route des Colles, 06903, Sophia Antipolis, France

* Corresponding author: pascal.biwole@uca.fr

Abstract

Straw is becoming a promising alternative insulation material to improve the building energy performance because of its low cost, large availability as cereal waste, its good hygrothermal properties, and its low embodied energy. The goal of this paper is to assess the hygrothermal performance of multi-layered straw walls with different boundary conditions. The study consists of evaluating five different straw-based wall assemblies, under a continental (Arkhangelsk, Russia), a tropical climate (Brasilia, Brazil), a temperate Mediterranean climate (Nice, France), and a cold desert climate Xinjiang (China). Numerical models of the heat and moisture transfer through the walls using WUFI software are developed, calibrated, and validated through experimental results from the literature. The chosen evaluation criteria are the total water content, the drying rate, the condensation risk, the mold growth, the moisture quantity, the time lag, and the decrement factor. Results show that straw walls with cement and/or wood covering can be used in tropical and temperate climates, coated straw walls with additional air layers in dry climates, while insulated straw walls are best fitted in continental climates. In the latter, the dryness rate varies between 7 and 40 % with a low condensation risk of value in the range of 0-12 %. It can be concluded that the straw wall's performance strongly depends on the interior and exterior added thermal insulation layers since they affect the ability of the material to dry out.

Keywords: Strawbale walls, bio-based material, hygrothermal modeling, simulation, energy efficiency

Highlights:

- The temperature and relative humidity variations obtained by WUFI are in good agreement with the literature experimental findings.
- The excessive moisture content in straw leads to bio-deterioration, mold, and decay damage in the whole structure.
- The hygrothermal issues in a straw wall depend on the interior and exterior covering layers.
- Hygrothermal issues can be solved by adding the straw thickness, adding a vapor retarder layer, adding an unventilated air layer, and controlling the indoor conditions.

Notations

ASH ASHRAE standard

CR	Condensation risk
DR	Dryness rate (%)
MC	Moisture content (%)
MG	Mold growth
RH	Relative humidity (%)
TWC	Total water content (kg/m ³)

Subscripts

int	interior
ext	exterior
max	maximum
min	minimum
B	Brasilia-Brazil
C	Xinjiang-China
F	Nice-France
R	Arkhangelsk-Russia

Nomenclature

f	Decrement factor (-)
H	Total enthalpy (J/m ³)
\varnothing	Relative humidity (%)
ϕ	Time lag (h)
w	Moisture content (%) (kg/m ³)
T	Temperature (K)
t	Time (s)
P _{sat}	Saturation pressure (Pa)
h_v	Evaporation enthalpy of water (J/kg)
D_{\varnothing}	Liquid conduction coefficient (kg/(m.s))
λ	Thermal conductivity (W/(m.K))
δ_p	Water vapor permeability (kg/(m.s.Pa))

1. Introduction

The use of agricultural products and their co-products for energy and industrial application is a topic of growing importance in the building construction and economic sector. Nowadays, sustainable products are becoming essential to preserve our planet. Cellulose fibers, straw fibers, wood, hemp fibers, and others are bio-based materials used for economic and ecological purposes. Straw with its characteristics showed multifunctional uses because it can be applied in the agriculture field for soil productivity [1], in the construction field to insulate the existing buildings or to construct new ones [2], and in pyrolysis reactions to convert biomass into alternative fuels or useful chemicals [3,4]. The United States Department of Agriculture's Economic Research Service [5] estimated the straw availability between 125 and 177 million tons each year from all types of grain. This estimation underlines the availability of straw as a material for construction.

Straw material has been used since the nineteenth century because of its known properties. It displays good thermal insulation [6,7], fire resistance [8], sound resistance [9,10] and a low energy consumption [11–13]. However, the main risks associated with the use of straw are the durability and stability of the building, due to moisture and condensation issues [14]. Mold growth, moisture presence, poor indoor air quality, loss of thermal resistance in wet insulation, material deterioration, and structural failure for load-bearing walls can all result from an improper envelope design [15]. An experimental setup in Germany [16] studied the performance of a straw wall covered by mud stucco. The thermal insulation property of the straw was shown by the temperature difference between the inner and outer surfaces. The inside surface temperature was varied between 10 °C and 18 °C when the exterior air temperature was between 2 °C and 23 °C. The relative humidity differences of both surfaces showed the same trend. The inside surface relative humidity was found about 60% when the outside relative humidity reached 70 %. The straw material was able to maintain the indoor conditions stable even when the exterior conditions were severe. Douzane *et al.* [17] measured the exterior and interior surface temperature and humidity of a plastered straw wall to assess its thermal behavior and the hygrothermal comfort level. They noticed that the interior surface temperature remained around 20 °C with relative humidity (RH) between 40-60 % when the exterior temperature was reaching its maximum of about 40 °C and its minimum of around -10 °C with RH between 30-90 %. Results showed that straw walls could decrease the temperature and RH fluctuations to maintain the indoor comfort conditions. The hygrothermal comfort of the building was also studied based on Fauconnier's model [18]. This model defines a comfort range by characterizing the couple temperature-humidity. The discomfort level reached a maximum value of about 32 %. Lawrence *et al.* [19] investigated the moisture content and RH variations of the straw material at a laboratory scale. The material was tested in a scientific oven by varying the temperature from 5 °C to 26 °C and the humidity from 33 % to 98 %. They found that the moisture content decreases when the temperature increases at maximum RH levels and rises to its maximum level when the RH is 98 %. Further research [20] compared the sorption isotherms of the flax, hemp, wheat straw, beech, and spruce fibers at 20 °C to see how they responded to changes in the building's interior environment. It was noticed that the plant fibers like wheat straw adsorbed about 45 % of moisture content (highest value) when reaching 95 % RH. The adsorption-desorption process of natural fibers showed the ability of the material to exchange moisture with its exterior, which prevents the material's and the building's degradation and provide indoor comfort.

The heat storage capability feature was also studied by calculating the time lag and the decrement factor for different envelopes. Douzane *et al.* [17] obtained about 6 h and 0.08 for a plastered straw wall for the time lag and the decrement factor, respectively. Gallegos-Ortega *et al.* [21] obtained about 9.12 h and 0.07 for another type of straw wall. The variation of results

from one study to another is related to the heat transfer coefficients of the wall, the different wall structure, the layers' thickness, and their thermal conductivity. The heat transfer coefficient of a wall in Montholier, France [22] covered by 2 cm of lime plaster on each side and having a total thickness of about 36.4 cm was found around 0.25 W/(m². K). The same structure composition was studied by Rye and Scott [23] for higher straw bale thickness of 43.5 cm. They obtained a U-value of about 0.16 W/(m². K) for the considered envelope. Cascone *et al.* [10] investigated a straw wall covered by wood and faux stone with unventilated air layers from both sides and determined a U-value of about 0.28 W/(m².K). The difference can also be explained by the variation of the straw thermal conductivity that varies according to the density of the sample, the fiber orientation in the bale, and the RH or moisture content. In general, the thermal conductivity of a straw bale can be as low as 0.033 W/(m.K) [24] and can reach up to 0.19 W/(m.K) [25]. Experiments showed that the thermal conductivity of the straw decreases when the density and RH decrease for bales having fibers perpendicular to the heat flow. All these factors are related to the amount of air in the porous material that gives an insulation feature leading to the use of a coupled heat and mass transfer model. Similar variations can be found for other thermo-physical parameters [26] such as the heat capacity with a listed range from 1338 J/(kg.K) to 2000 J/(kg.K), the thermal effusivity with a range between 417 J/(K.m².s^{1/2}) and 775 J/(K.m².s^{1/2}) and the diffusivity that ranges between 10⁻⁷ m²/s and 3.6 x 10⁻⁶ m²/s. These aspects illustrate the capability of the material to accumulate and exchange heat.

Many researchers have determined the hygrothermal properties of straw walls by monitoring the temperature and RH variation through the wall over a short period and by defining and calculating parameters that show its capability to store heat. In addition, they focused on the thermal conductivity of straw-based on experimental measurements of bales. However, no study was found reporting the dryness rate of a wall or the mold growth within its structure and proposing the best wall structure according to the exterior and interior boundary conditions. Developing a complete investigation concerning the moisture transfer in the straw walls should consider a wide range of criteria since moisture has several sources and transport mechanisms. The present paper evaluates the hygrothermal behavior of five typical multi-layered straw-based walls under the weather conditions of four locations. First, a numerical model of the transient heat and mass transfer in the walls is set up using WUFI[®] software [27], one of the most used and validated hygrothermal simulation tools. For validation purposes, the simulated results of temperature and RH through the wall are compared with experimental data found in the literature [17]. Since many uncertainties exist in the straw thermophysical properties due to the biodegradable nature of the material, a calibration is carried out on the model using parametric analysis and experimental data. Then, the relevant material properties and straw wall assemblies are collected from the existing literature and the typical climate conditions are selected based on the heterogeneity of their seasonal precipitations, solar irradiation intensities, as well as the availability of the cereal production. Afterward, the hygrothermal performance of the five straw walls types is investigated. The results are presented based on different assessment criteria, namely total water content, mold growth, heat losses, drying rate, condensation risk, time lag, and decrement factor. Finally, the main findings of the study are discussed and compared with the existing literature. New wall assemblies are proposed to solve some issues in the hygrothermal behavior revealed by the simulated results. Last, the required future research is identified to complete the existing knowledge.

2. Modeling approach

2.1. Numerical model

The physical model is that of multi-layer walls under transient boundary conditions. A numerical model based on WUFI software is used to predict the hygrothermal response of the

walls under different weather conditions. WUFI-2D, developed by the Fraunhofer Institute for Building Physics in Germany, is a hygrothermal simulation program to analyze and perform the heat and moisture transfer in 2D construction envelopes. The software introduces two moisture-flow driving forces: the liquid transport flux, which is affected by relative humidity, and the vapor diffusion flux, which is affected by vapor pressure. Conductive heat transfer, enthalpy flow, solar radiation (long and short waves), and surface diffusion (for the water movement) are all part of the equation [28,29]. WUFI solves the temperature equation and the moisture equation iteratively, updating the storage and the transport coefficients in each iteration to the new moisture and temperature fields until convergence is reached. The energy transfer equation and the moisture transfer equation are shown in equations (1) and (2), respectively.

$$\frac{\partial H}{\partial T} \cdot \frac{\partial T}{\partial t} = \nabla \cdot (\lambda \nabla T) + h_v \nabla \cdot (\delta_p (\phi P_{sat})) \quad (1)$$

$$\frac{\partial w}{\partial \phi} \cdot \frac{\partial \phi}{\partial t} = \nabla \cdot (D_\phi \nabla \phi + \delta_p \nabla (\phi P_{sat})) \quad (2)$$

where H , T , w and ϕ are enthalpy, temperature, moisture content, and relative humidity, respectively. P_{sat} , λ , h_v , δ_p and D_ϕ are the saturation pressure, thermal conductivity, evaporation enthalpy of water, water vapor permeability, and liquid conduction coefficient, respectively.

The left side of equation (1) represents the thermal inertia while the terms on the right side are respectively the thermal diffusion and the liquid and vapor convection. In equation (2), the left side represents the moisture storage while the liquid diffusion and the vapor diffusion are respectively modeled on the right side. WUFI solves these equations by using the finite volume technique and a fully implicit scheme for spatial and time discretization. The model input parameters include the wall geometry, the materials properties, the outdoor and indoor weather data, the initial conditions (T , RH), and the calculation period. Several researchers used WUFI to assess the hygrothermal behavior of building exterior walls. Mesa and Arenghi [30] validated their WUFI numerical model using experimental results from testing a straw bale wall in a climatic chamber. Kalamees and Venha [31] compared different programs, 1D-HAM, MATCH, and WUFI-2D with experimental results to compute the hygrothermal performance of timber-framed wall structures. Those comparisons gave similar results, which proved that WUFI is a useful tool to assess the moisture behavior of a wall.

The following section presents the numerical model validation, based on a straw wall experimentally studied by Douzane *et al.* [17].

2.2. Model validation

Douzane *et al.* [17] studied the hygric and thermal behavior of a two-story straw bale building with a total floor area of 188 m². The ground floor is composed of an open area and three rooms. The upper floor is divided into three bedrooms. The building external walls' layout is shown in **Figure 1**. It is composed of 35 mm of exterior lime plaster, 440 mm of straw layer, 30 mm of the unventilated air layer, and 15 mm of plasterboard.

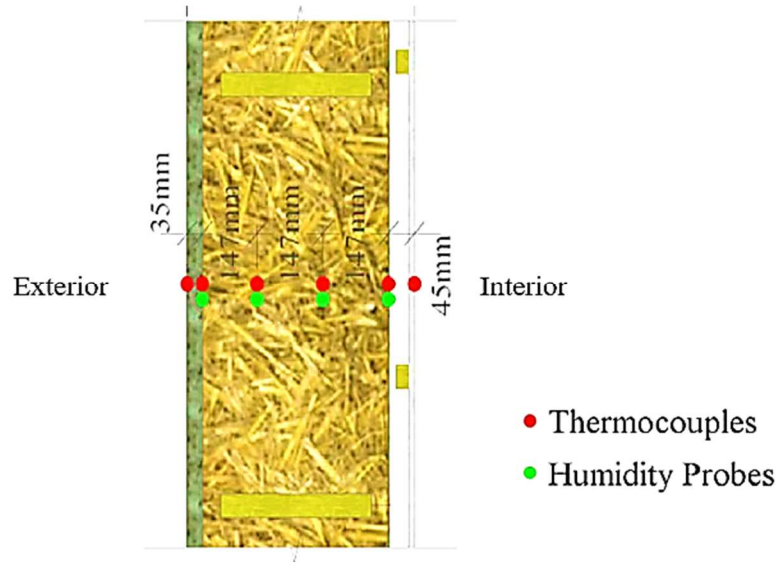


Figure 1: Location of thermocouples and humidity probes in the straw wall [17]

Straw characteristics are variable regarding its thermal properties that depend on the straw type, density, water content, relative humidity, wall thickness, and fibers' orientation. WUFI contains a large material database that distinguishes between basic hygrothermal values and hygrothermal functions. The constant parameters for the non-steady computation of the temperature fields at 20 °C and 20% RH are the bulk density of the dry material, specific heat capacity, and thermal conductivity. For both hygroscopic and non-hygroscopic materials, basic hygric parameters such as the water vapor diffusion resistance factor and porosity must be provided. Other hygric properties include the thermal conductivity variation based on the moisture content and the thermal conductivity based on temperature variations. On the other hand, moisture storage function and the moisture-dependent liquid transport coefficient are needed for hygroscopic and capillary material simulation, respectively. The variations of each parameter must be entered to study their effect on the whole structure.

The thermophysical properties of lime plaster, unventilated air, and plasterboard taken from the WUFI database are provided in **Table 1**. Straw samples with dimensions of 50×50×10 cm³ and a density of 80 kg/m³ were evaluated for thermal conductivity using a guarded hot plate apparatus after being oven-dried at 65 °C. Experiments showed that for bale average temperature between 10 °C and 40 °C, the thermal conductivity varied between 0.067 W/(m.K) and 0.088 W/(m.K) for horizontal fibers and between 0.046 W/(m.K) and 0.064 W/(m.K) for vertical fibers. The U-value of the experimental straw wall has about 0.2 W/(m².K).

Table 1: Straw buildings materials basic properties extracted from WUFI materials database and literature at 20 °C and 20 % RH

Material	Thermal conductivity (W/(m.K))	Density (kg/m ³)	Specific heat (J/(kg.K))	Porosity (m ³ /m ³)	Water vapor diffusion resistance factor (-)
Straw [17]	0.046-0.088	80	1200	0.9	1.3
Unventilated air gap (30 mm)	0.2	1.3	1000	0.99	0.32
Plasterboard	0.2	850	850	0.65	8.3
Lime plaster	0.7	1600	850	0.3	7

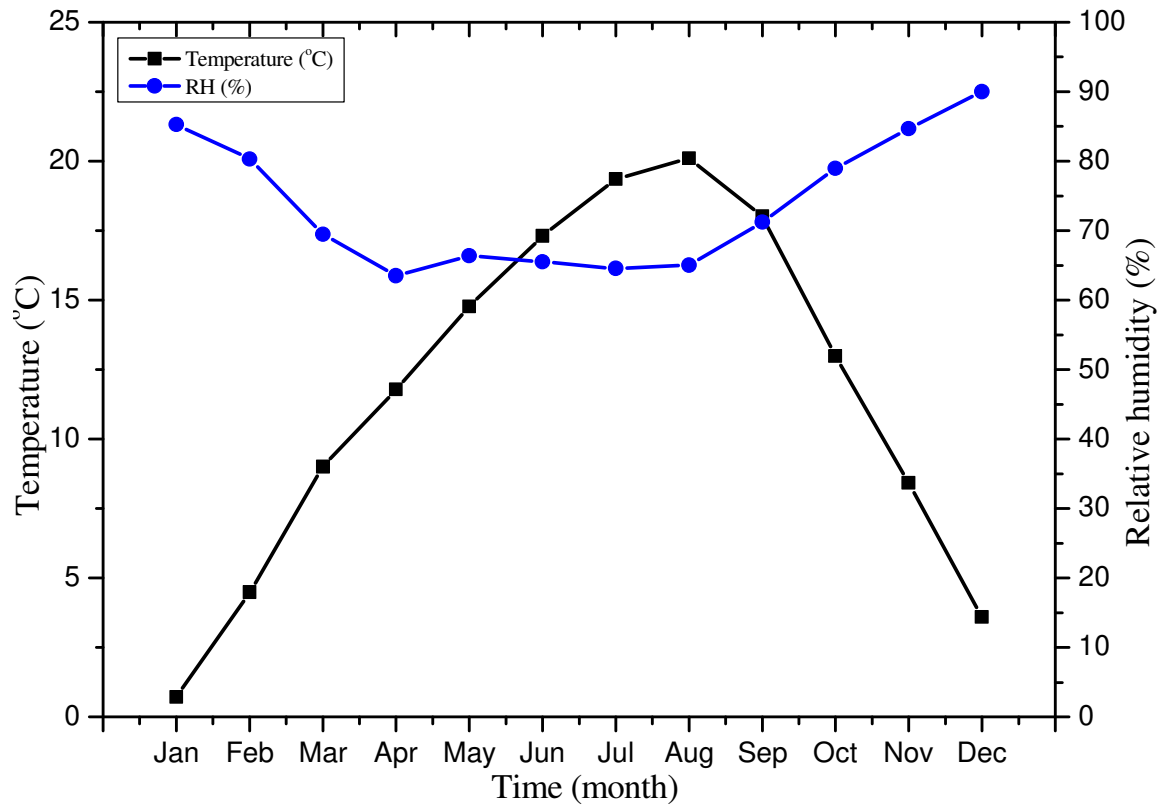


Figure 2: Monthly average outdoor temperature and relative humidity in the Picardy region

The tested building is situated in the Picardy region, north of France. The Picardy climate is classified as temperate oceanic (Cfb) by the Köppen–Geiger classification [32]. The outdoor dry air temperature reaches 40 °C in summer and -10 °C in winter. **Figure 2** shows the monthly average outdoor temperature and RH in the test location. The outdoor RH ranges between 30 % in summer and 90 % in winter. The building indoor temperature and RH were maintained between 20-25 °C and 40–60 % respectively, to ensure indoor thermal comfort. The authors measured the temperature and the RH at 38 different locations in the building using type-T thermocouples and HMP60 humidity probes. Inside a wall assembly, the distance between sensors was around 147 mm as shown in **Figure 1**. The experiment took place for 14 months between 25 May 2014 and 11 August 2015.

Figure 3 shows the experimental temperature and the RH variation of the outer and inner surface of the south-facing wall during the test period. The graph reveals the stability of the internal surface temperature at around 20 °C, even when the external surface temperature is very low or very high. The internal surface RH varies between 30 % and 60 % and does not depend on the large RH variation of the external face. The lower values of the inner surface RH can be explained by the heating of the building during winter, which increases the capacity of ambient air to store moisture without reaching saturation. Douzane *et al.* [17] concluded that the straw envelope could mitigate the outdoor temperature and moisture variations to preserve indoor comfort during the summer and the winter periods.

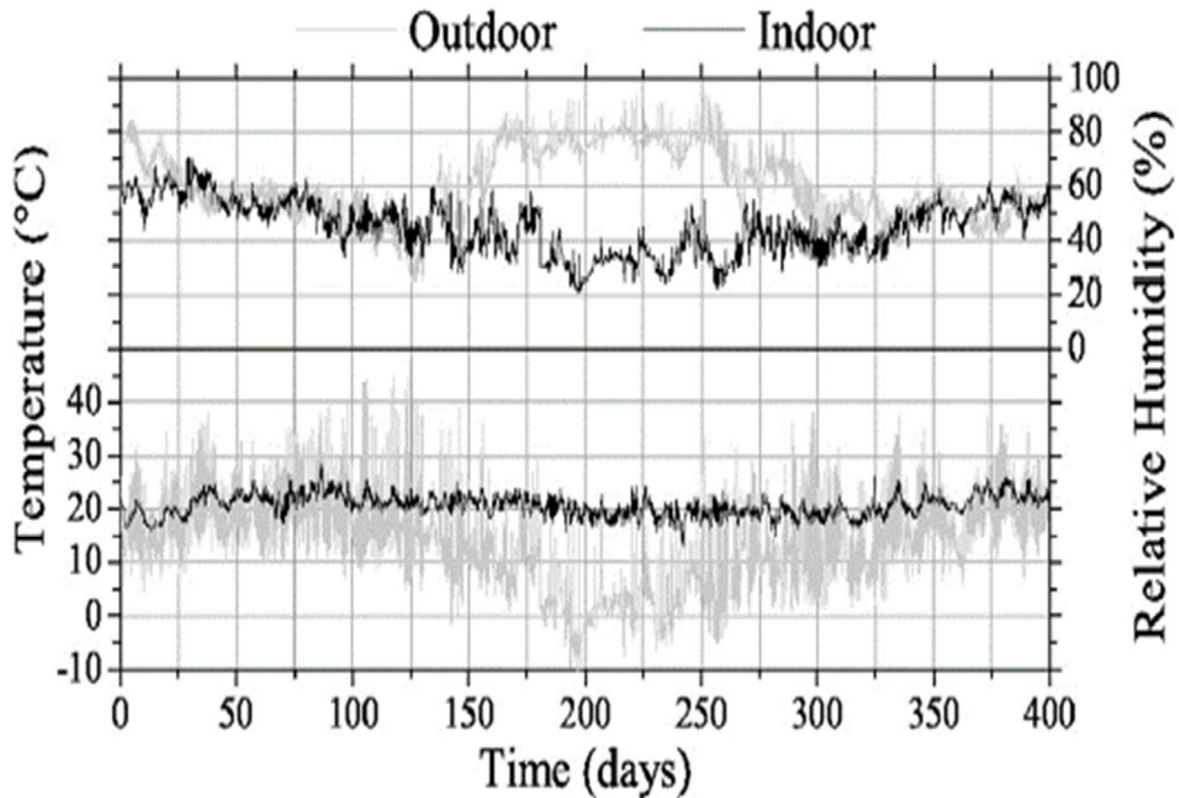


Figure 3: The variation of the inner and outer surfaces temperature and RH [17]

The experimental data of [17] was used to calibrate and validate the numerical model by comparing the profile of the measured data to that of the simulated results for the internal and external surface temperatures and RH over one year. Therefore, a WUFI model was set up using a geometry and weather data file similar to that of **Figure 2** and **Figure 3**, respectively. In the model, the interior surface's heat transfer coefficient was considered $8 \text{ W/m}^2\text{K}$ with a short wave radiation absorptivity of 0.2 and longwave radiation emissivity of 0.9 regarding its bright color. The heat transfer coefficient of the exterior surface was considered wind-dependent with a short-wave radiation absorptivity of 0.6 and longwave radiation emissivity of 0.9. Based on the initial exterior and interior air temperature and RH, the initial temperature was set at $20 \text{ }^\circ\text{C}$ for all materials and the initial RH was set at 50 % for straw, wood boards, and plasterboards and 80 % for lime plasters.

To obtain hygrothermal numerical results comparable to the experimental data, a calibration technique was required due to some experimental uncertainties. The simulation was replicated for different values of outer surface solar absorption, straw initial water content, and straw thermal conductivity, until reaching a high accordance between the simulated and experimented surface temperature and RH variations. The straw thermal conductivity was finally set to 0.055 W/(m.K) at $20 \text{ }^\circ\text{C}$ and 20 % RH. The straw initial relative humidity was set at 40 %. The heat transfer coefficient of the interior surface was varied between 2 and $10 \text{ W/(m}^2\text{.K)}$ and fixed at the end at $8 \text{ W/(m}^2\text{.K)}$. The unmeasured moisture straw sorption isotherm and the variation function of straw thermal conductivity versus temperature and RH were collected from literature [25], [28], [29], as shown in **Figure 4**. These graphs provide information about the variation of the insulating property of the straw as a function of temperature and RH as well as the material's adsorption isotherm. High temperature and humidity affect negatively the thermal conductivity of the straw. The conductivity increases progressively with the temperature and reaches about 0.065 W/(m.K) at $45 \text{ }^\circ\text{C}$. At the same time, the thermal conductivity increases with the RH until reaching 0.06 W/(m.K) at 80 % RH and then continues rising sharply to

attain 0.12 W/(m.K) at 100 % RH. As for the moisture content variation, the graph shows its progressive raise while increasing the RH. This behavior demonstrates the high porosity of the straw.

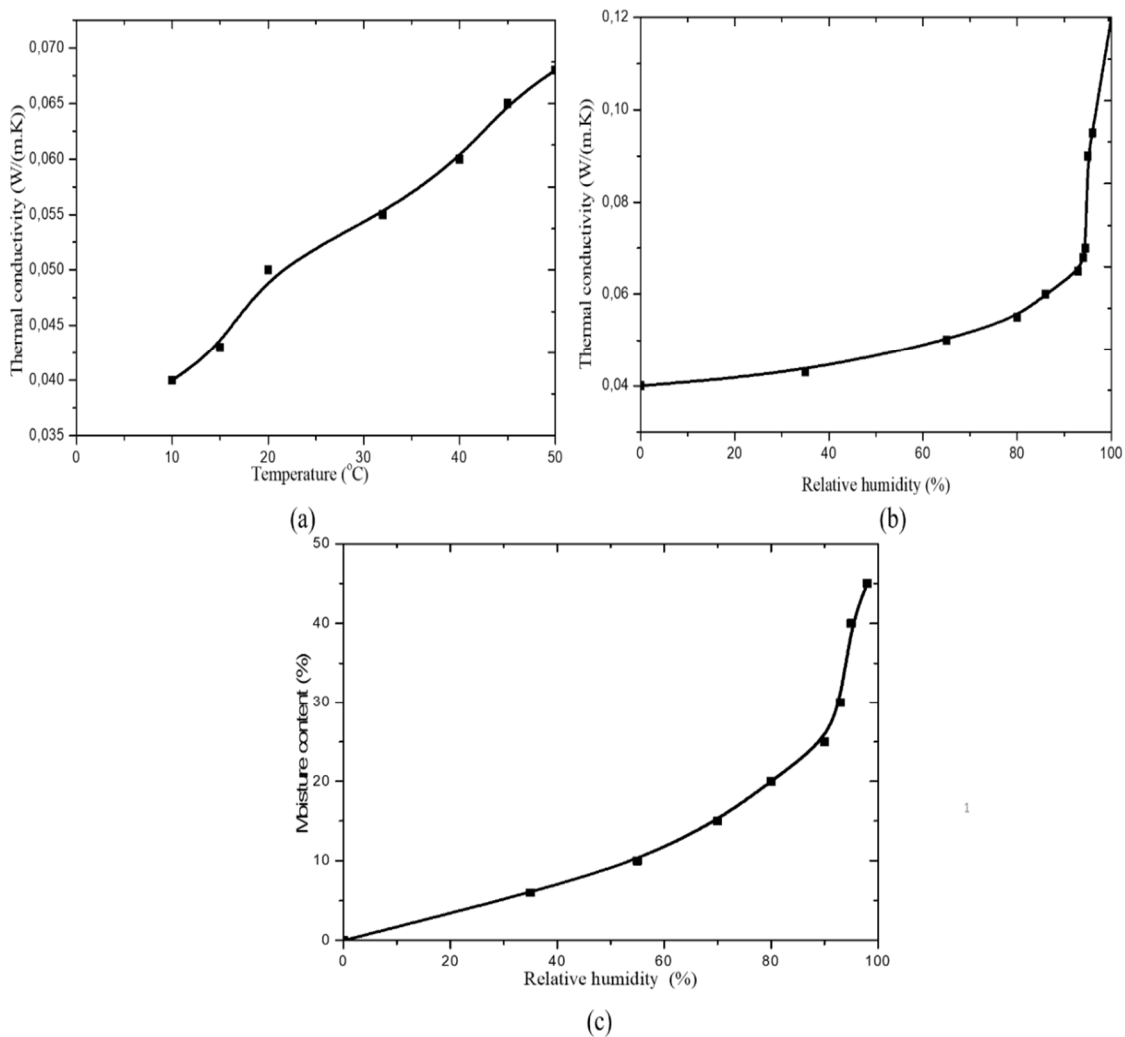


Figure 4 : Hygrothermal functions showing the thermal conductivity-temperature variations (a), the thermal conductivity-relative humidity variations (b) and the moisture content- relative humidity variations (c) for the straw material (based on [17], [25], [28], [29])

The weekly-averaged experimental and simulated results showing the temperature and the RH of the interior and exterior surfaces are represented in **Figure 5** and **Figure 6**, respectively. The WUFI model generates almost similar results as the experimental study of the straw building for the studied weather conditions. The peaks in the simulated case and the variation of values are close to the measured data. Regarding temperature, the plotted values are in good agreement with the measured values. The maximum obtained temperature for the exterior wall surface reaches 45 °C in the simulation results while it reaches about 43 °C in the experimental measurements. The minimum calculated temperature is about -14 °C while it is -10 °C in the experimental measurements. The interior surface temperature varies around 20 °C, which agrees with the experimental results.

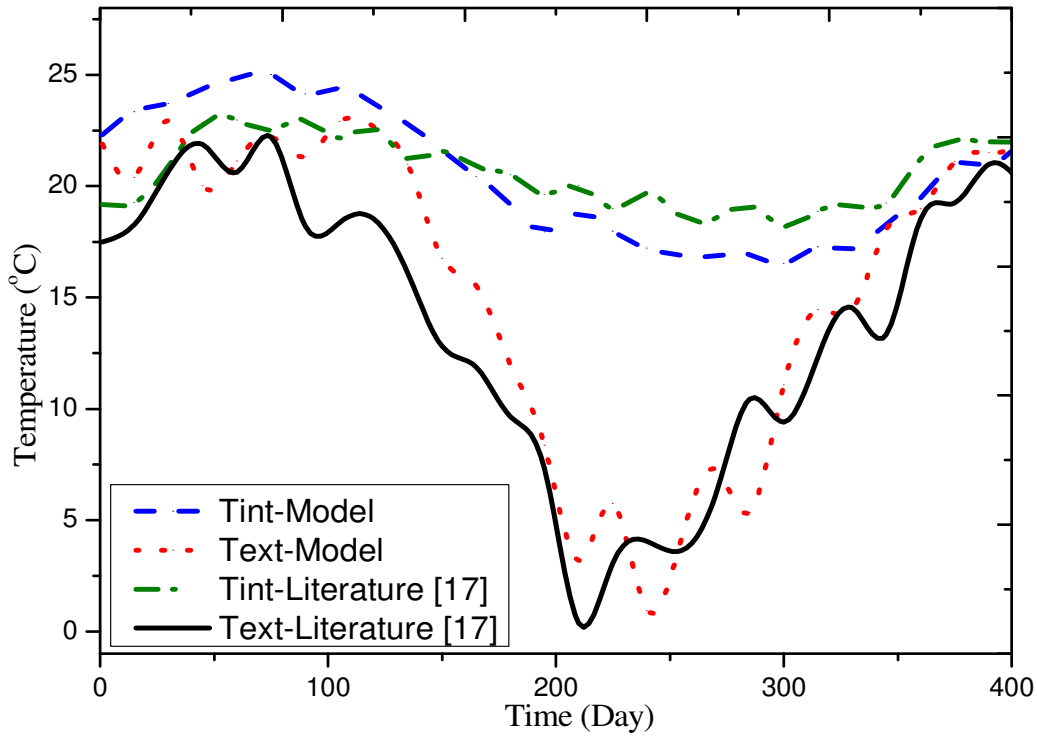


Figure 5: The temperature weekly average variation over one year for the third wall simulated in WUFI under Picardie weather conditions.

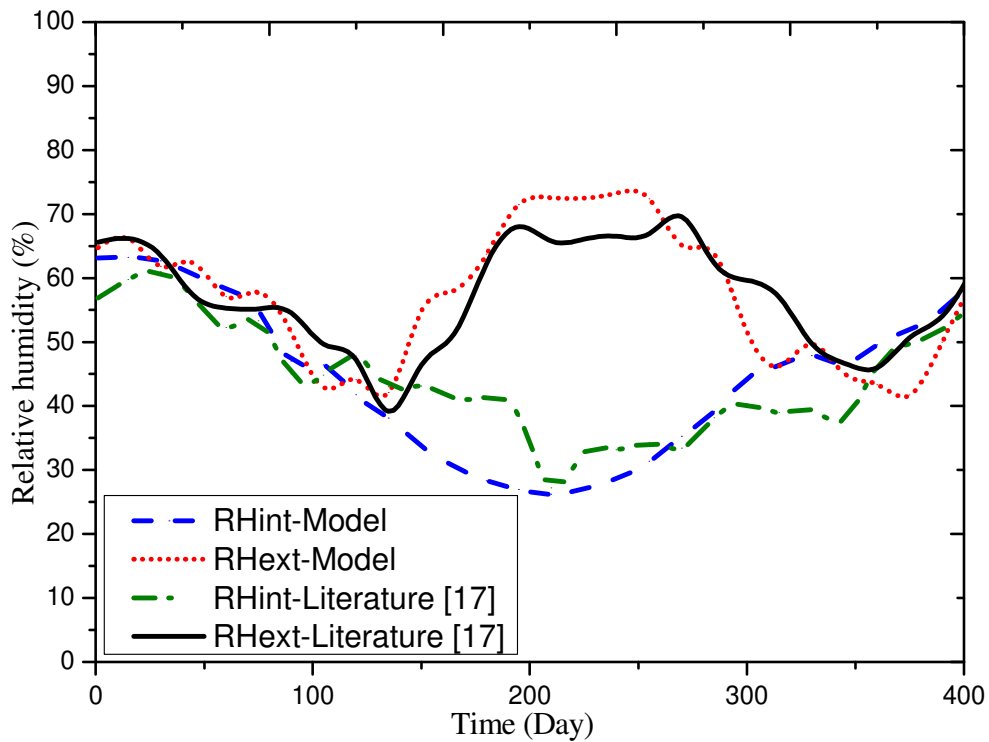


Figure 6: The relative humidity weekly average variation over one year for the third wall simulated in WUFI under Picardie weather conditions.

Besides, the RH variation of the wall surfaces compares well to the experimental results. The initial value for RH considered in the numerical model (for the numerical case, the initial RH for the straw and wood is 40 % and 80 % for the lime plaster) can explain the differences in the interior surface RH variation. The behavior of the exterior surface RH is close to the in-situ

measurements. The interior surface humidity varies between 35 % and 60 % while the exterior surface humidity varies between 25 % and 85 %.

Douzane *et al.* [17] calculated the thermal inertia parameters based on the exterior and interior surface temperature variations for 24 hours to prove the mitigating effect of the straw-based wall against external variations and its beneficial impact on indoor thermal comfort. The time lag and the decrement factor are given in equations (3) and (4), respectively [35].

$$\phi = t_{int,max} - t_{ext,max} \quad (3)$$

$$f = \frac{T_{int,max} - T_{int,min}}{T_{ext,max} - T_{ext,min}} \quad (4)$$

where $t_{int,max}$ and $t_{ext,max}$ are the time when the interior temperature and the exterior temperature, respectively, are at their highest values. $T_{int,max}$, $T_{int,min}$, $T_{ext,max}$ and $T_{ext,min}$ are the maximum and minimum temperatures of the internal and external surfaces.

The experimental results indicate a time lag of about 6 h and a decrement factor of about 0.09 while the numerical results show a time lag of about 7 h and a decrement factor of about 0.066. **Figure 7** shows that the variation of the outdoor surface temperature barely affects the indoor surface temperature variation. For the numerical model, the difference between the maximum and the minimum of the external temperature was about 30 °C, which is close to the measured values. However, the temperature range of the internal surface is about 1.3 °C for the numerical model and 3 °C for the experimental measurements. The discrepancy between actual and modeled materials characteristics and initial conditions can explain this difference. These results prove the thermal resistance of the straw bale wall that helps limit the overheating in summer since the highest interior temperature is reached when the exterior temperature has decreased.

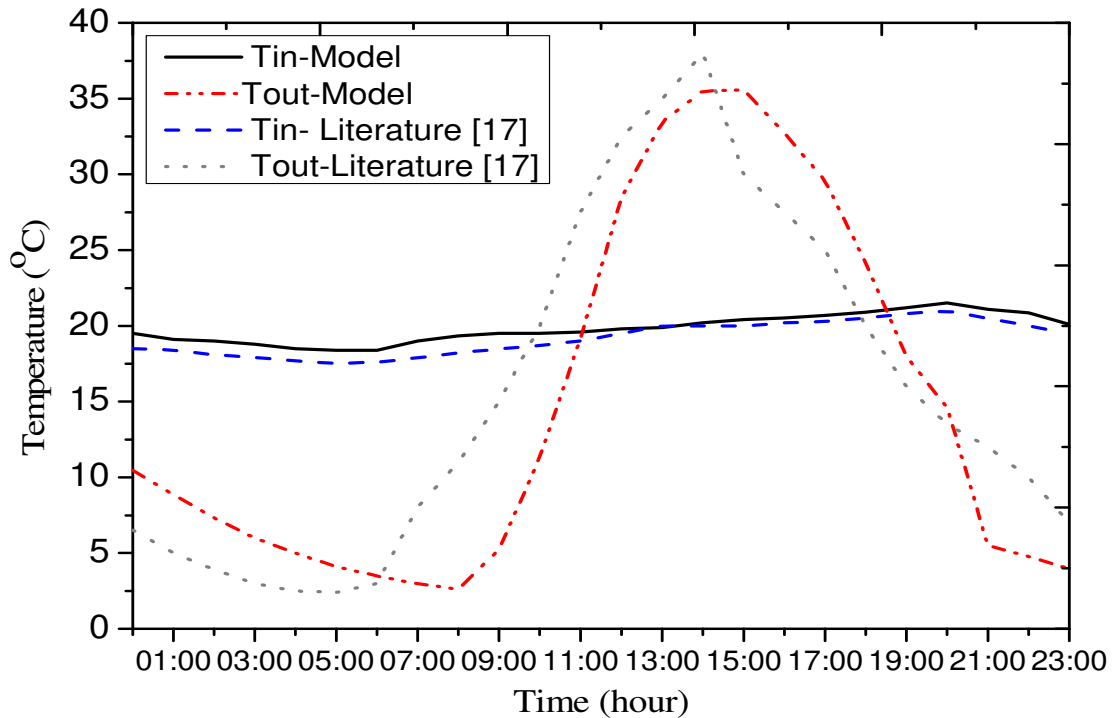


Figure 7: The variation of the interior and exterior surface temperature for the numerical model (WUFI) and the experimental model (Literature [17]) for 24 hours on 25 April

The root mean square error (RMSE) and the percentage root mean square error (PRMSE) indicated in equations (5) and (6), respectively, are used to measure the agreement between experimental data (e_i) and simulated outcomes(s_i).

$$RMSE = \sqrt{\frac{1}{n} \sum_{i=1}^n (s_i - e_i)^2} \quad (5)$$

$$PRMSE = \sqrt{\frac{1}{n} \sum_{i=1}^n \left(\frac{s_i - e_i}{e_i} \right)^2} \times 100 \quad (6)$$

The RSME and PRSME of the exterior surface temperature are 1.6 °C and 9 % respectively, while those for the interior surface temperature are 1 °C and 3.6 %, respectively. The RSME and PRSME of the exterior surface RH are 2 % and 3.5 % respectively, while those for the interior surface RH are 2.2 % and 4 %. These values quantitatively show the good agreement between the numerical and the experimental models. The numerical model is therefore used in the following section to investigate different wall configurations.

3. Case study

3.1. Materials properties

The principal layer in straw bale walls is the straw layer with a thickness varying from 360 mm to 440 mm. Strawbale walls are covered on both sides with cement or lime plasters and wood boards. All material properties including thermal conductivity, porosity, water vapor diffusion resistance factor, specific heat, and density are presented in **Table 2**. The layers' characteristics are taken from the WUFI database except for the straw. The straw characteristics are collected from different research works [17], [25,33,34]. The straw hygrothermal functions for moisture storage and thermal conductivity versus temperature and RH are taken the same as in **Figure 4**.

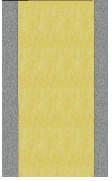



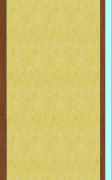
Table 2: Straw buildings materials basic properties extracted from WUFI materials database and literature at 20 °C and 20 % RH

Material	Thermal conductivity (W/(m.K))	Density (kg/m ³)	Specific heat (J/(kg.K))	Porosity (m ³ /m ³)	Water vapor diffusion resistance factor (-)
Cement plaster	1.2	2000	850	0.3	25
Hardwood board	0.13	650	1500	0.47	200
Wood wool	0.08	450	1500	0.55	9
Straw [25], [28], [29]	0.055	120	1200	0.9	1.3
Unventilated air gap (30 mm)	0.2	1.3	1000	0.99	0.32
Unventilated air gap (50 mm)	0.28	1.3	1000	0.99	0.32

3.2. Wall configurations

The numerical model is applied to study five different wall structures under four different weather conditions. Straw construction is found in different forms and structures depending on the prevailing climate at the building's location. **Table 3** gives the most used wall structures in the actual straw construction sector.

Table 3: Different layers composition of five considered cases

Cases	Exterior layer-----				-----Interior layer			
	Layer 1	Layer 2	Layer 3	Layer 4	Layer 5	Layer 6	Layer 7	Layer 8
Case 1 [36] 	Cement plaster 20mm	Straw 360mm	Cement plaster 20mm	-	-	-	-	-
Case 2 [8] 	Hardwood 30mm	Straw 360mm	Hardwood 30mm	-	-	-	-	-
Case 3 [17] 	Cement plaster 35mm	Straw 440mm	Unventilated air gap 30mm	Hardwood 15mm	-	-	-	-
Case 4 [37] 	Hardwood 40mm	Unventilated air gap 30mm	Cement plaster 20mm	Straw 360mm	Cement plaster 20mm	-	-	-
Case 5 	Cement plaster 10mm	Wood wool 40mm	Hardwood 18mm	Straw 360mm	Hardwood 10mm	Unventilated air gap 50mm	Hardwood 30mm	Cement plaster 15mm

In the first wall structure, a 20 mm thick cement layer covers the straw from both sides and gives a total wall thickness of around 400 mm. Cement plaster is used as a surface finish to protect the straw from fire, rot, and fungus, even though this material increases the carbon footprint of the wall [38]. In the second case, 30 mm hardwood boards cover the straw layer on both sides, thus yielding a wall assembly thickness of 420 mm. Hardwood boards are used to protect the straw layer, to increase thermal performance, and reduce the environmental impact of the wall in the condition that the wood source is sustainably exploited [39],[40]. In the two following cases, an unventilated air layer is added at different positions to increase the insulation property of the wall, reduce the mass transfer, and provide space for electrical cables and pipework. The thickness of the straw is different in those two cases, as well as the total wall thickness, which is 520 mm and 470 mm in case 3 and case 4, respectively. Those two walls can show the effect of the straw thickness and the air layer on the hygrothermal properties of the whole structure. In the last case, a wood wool layer was added to increase the thermal resistance of the wall. The total thickness of the structure is 533 mm. The latter assembly was recently proposed by French contractors [41] to increase the thermal comfort in straw buildings.

Parameters such as solar radiation, the driving rain intensity and direction, and the structure orientation affect the hygrothermal behavior of the wall. It is important to study the worst-case scenario of an envelope exposed to the highest hygrothermal stress. Therefore, all walls in the present study are north-oriented, since the generally higher driving rain intensity and lower solar radiation in that direction increase the occurrence probability of drying problems.

3.3. Climates

3.3.1. Outdoor climates

Four climates were chosen according to their extremely different temperature and humidity profiles, as reported by the Köppen–Geiger classification [32], and according to cereal availability. The cost and the environmental impact of the construction caused by the material transportation from the manufacturing location to the site of work are thus minimized. The USA, China, Russia, Brazil, and some European countries have the highest annual cereal production [42]. Therefore, the cities chosen in this study are Nice-France, Xinjiang-China, Arkhangelsk-Russia, and Brasilia-Brazil. **Table 4** describes the main weather characteristics of the selected cities as well as their longitude, latitude, and elevation. Tropical, dry, temperate, and continental climates were considered to test the ability of straw walls to stabilize the interior variation of the temperature and relative humidity.

Not all these areas experienced growth in straw construction. In the Russian region, construction with straw bales was started in 1996 by foreign organizations as an experimental environmental village. This type of construction has since been developed in Belarus, Ukraine, and Russia [43,44]. In the Brazilian construction field, straw buildings were first utilized in the 1970s, but their use declined in 2009 and are not widely used today [45]. Straw buildings appeared in China's construction industry in 1998. More than 600 straw structures have been constructed in China since then [46]. In France, more than 4000 buildings are constructed from wheat straw bales [47]. Straw bale construction attracts growing interest in the industrial sector, regarding its sustainability, its practicality, and its reduced construction time.

Table 4: Köppen–Geiger Climate classification for the four chosen cities

City, Country Climate	Location	Description
Brasilia, Brazil Aw	Longitude= 47.93 west Latitude= 15.78 south Height=1160 m Time zone= -3	<ul style="list-style-type: none"> • Tropical wet and dry or savanna climate • Dry winter • Average temperature about 18°C
Xinjiang, China BWk	Longitude= 89.2 east Latitude= 42.93 north Height=35 m Time zone= +8	<ul style="list-style-type: none"> • Cold desert climate • Average temperature below 18°C • At least one month has a temperature below 0°C
Nice, France Csa	Longitude= 7.2 east Latitude= 43.65 north Height=10 m Time zone=+1	<ul style="list-style-type: none"> • Temperate and Mediterranean climate • Precipitation in winter, dry and hot summer • Average temperature above 22 °C
Arkhangelsk, Russia Dfc	Longitude= 40.47 east Latitude= 64.53 north Height=13 m Time zone= +4	<ul style="list-style-type: none"> • Subarctic continental climate • No dry season and cold summer • Maximum average temperature 10 °C

Figure 8 presents the outdoor temperature and RH of each climate. The Figure shows remarkable differences between cities' temperature and RH variations. In Brasilia, the maximum temperature is generally reached in September, the warmest month of the year with a monthly average temperature of about 21.5 °C. The minimum average temperature reaches about 18 °C in the coldest month, July. The average RH varies between 40 % and 88 %, respectively in September and in December. It should be noted that December is the wettest month while July is the driest one. In Xinjiang, the warm season is from May to September where the maximum weekly average temperature reaches about 33 °C with a low RH of about 30 %. The cold season is from November to January where the monthly average temperature reaches -12 °C with a high RH of about 80 %. The wettest month in Xinjiang is January and the driest month is July. In Nice, the warmest month is August with a maximum weekly average temperature of about 25 °C and an RH reaching about 75 %. The coolest month is December with a minimum average temperature of about 6 °C where the RH reaches about 50 %. In general, the wettest month in Nice is November and the driest month is July. In Arkhangelsk, the extreme weekly average temperatures are about 17 °C and -17 °C, respectively in July the hottest month and in January the coldest month. The humidity varies between 60 % and 90 % for the same months. The wettest month is February and the driest one in August. The weather data files are extracted from the EnergyPlus weather library [48].

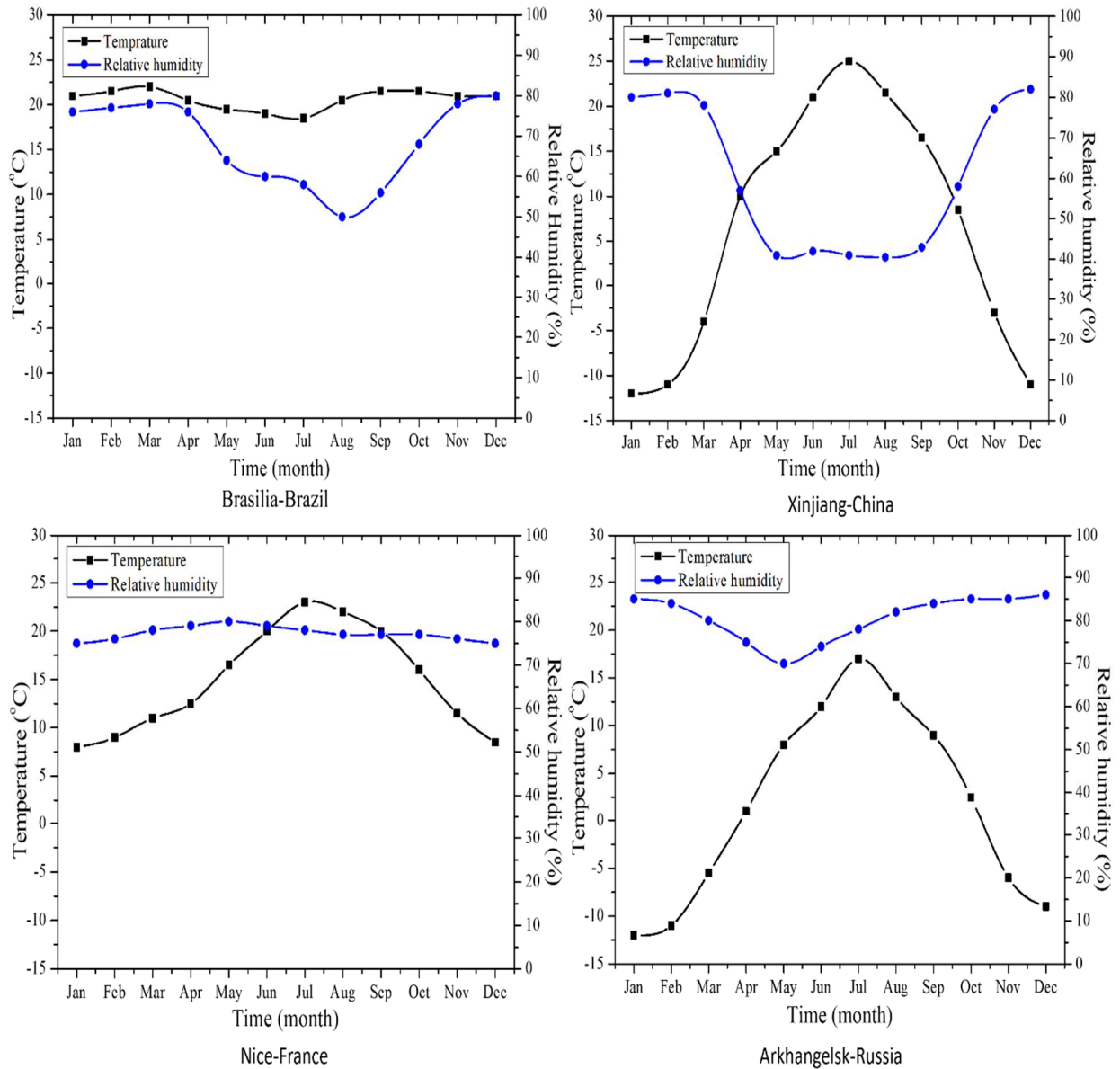


Figure 8: Monthly average outdoor temperature and relative humidity in Brasilia-Brazil, Xinjiang-China, Nice-France, and Arkhangelsk-Russia over one year

3.3.2. Indoor climates

The simulated sinusoidal function for the temperature and the humidity is respectively given in equations (7) and (8).

$$T = 2.5 \sin(t - c) + 21.5 \quad (7)$$

$$RH = 10 \sin(t - h) + 50 \quad (8)$$

where t is the time (month), c and h are constants that depend on the climate characteristics of the considered region, as shown in **Table 5**. The resulting temperature and RH graphs are plotted in **Figure 9**. The indoor dry air temperature ranges from 19 °C (winter) to 24 °C (summer) while the indoor RH varies between 30 % (winter) and 60 % (summer). These variations are based on ASHRAE-55 [49] and EN 13779 [50] which recommend a winter

temperature of 19 °C to 24 °C with a relative humidity of 30-40 %, and a summer temperature of 23 °C to 26 °C with a relative humidity of 50-60 %.

Table 5: c and h values used in equations (7) and (8) for each country

Country	c	h
Brazil	2.57	-2
China	1.57	-1.57
Nice	2	0.57
Russia	1.57	-2.57

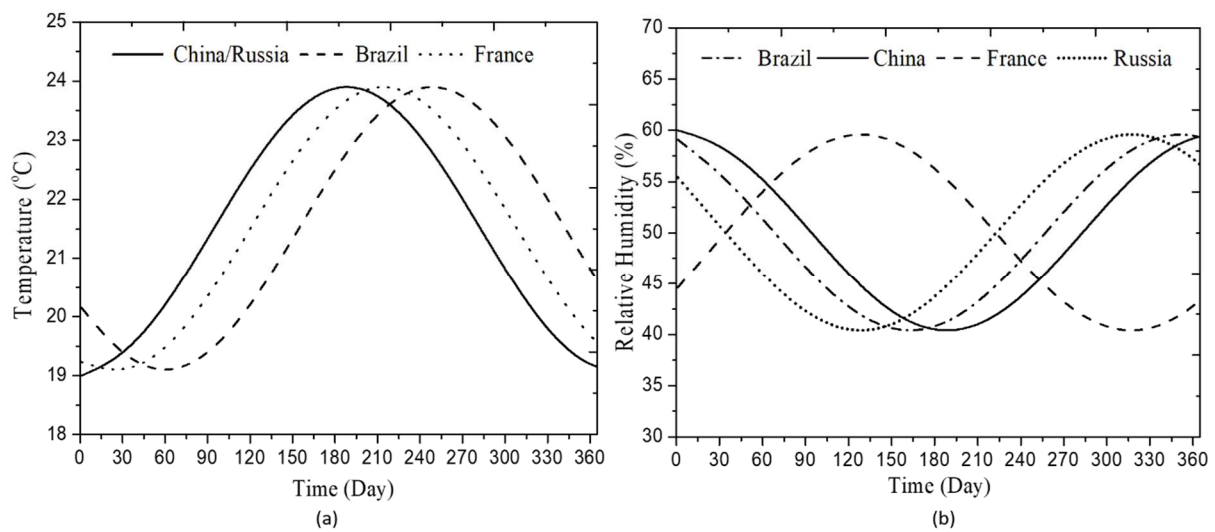


Figure 9: Annual variation of the indoor dry air temperature (a) and the indoor air relative humidity (b)

3.4. Hygrothermal criteria

In the present study, the thermal evaluation uses the time lag and the decrement factor, as presented in equations (3) and (4), to detect respectively the time that takes a heatwave to cross the wall and the decreasing ratio amplitude. The hygric evaluation uses the following criteria:

- Total water content (TWC): its variation shows the capacity of the wall to dry out over 4 years. This can be evaluated by comparing the initial and the final moisture content. The wall passes this criterion if the final content is lower than the initial content.
- Dryness rate (DR): a higher dryness rate means increased ability to dry out. The DR calculates the difference between the final and initial moisture content.
- Condensation risk (CR): On the indoor surface, the condensation risk appears if the material temperature is lower than the indoor dew point temperature [51]; this risk will be greater if this case period appears for a long time. For each wall, the percentage of time the surface temperature falls below the dew point is determined. Within the wall, the CR appears when the calculated vapor pressure is higher than the saturated vapor pressure.

- Mold growth (MG): Mold can grow when the hygrothermal conditions of a wall reach a particular threshold. This limit known as the lowest isopleth for mold (LIM) is based on humidity, temperature, exposure period, and material properties. The criterion consists of plotting the RH of a material versus the temperature at a certain time. As a result, if the conditions (RH and T) remain over the LIM for an extended period, the building material will be prone to grow mold. For building materials, two limitations LIM 1 and LIM 2 are of interest. The first is for products created from biodegradable materials, while the second is for non-biodegradable materials.
- ASHRAE criterion (ASH): The ASHRAE criterion was created to prevent moisture problems in envelope assemblies by limiting the amount of moisture in buildings[52]. The standard can be applied to all materials and surfaces except for the external layers. To avoid mold development after 30 days with an average surface temperature between 5 °C and 41°C, the standard demands a time-averaged surface RH of less than 80 %.

Those criteria have been used by several authors [15], [53,54] to assess the hygrothermal performance of walls. Based on WUFI results, they are utilized to analyze the behavior of five typical straw wall assemblies in the next section. Moisture concerns are predicted for all cases under various boundary circumstances through these findings.

4. Results and discussion

The five cases of straw walls proposed in **Table 2** are considered to find the optimum assembly depending on the four chosen locations around the world. Knowing that the initial condition in WUFI can be modified according to each material, the RH and the temperature of the straw and the wood were respectively considered equal to 50 % and 20 °C, while for the other material they were set to 80 % and 20 °C. In all cases, the wall was oriented to the north where the solar radiation is low and the driving rains are high. The WUFI outputs show the variation of the water content, the relative humidity, and the temperature of each layer with respect to time. The analysis of the walls' behavior is based on WUFI outputs and hygrothermal criteria. The objective of the simulations is to detect risks of condensation, problems of dryness, and mold growth for each climate, to choose the optimal wall design for each area, or to propose novel wall layouts.

4.1. Total water content

Excessive moisture content in straw and hygroscopic building materials leads to bio-deterioration, mold, and decay damages in the whole structure. **Figure 10** compares the day-averaged total water content variation for wall cases three, four, and five Arkhangelsk-Russia and Brasilia-Brazil over four years. The graphs depict different outcomes depending on the studied cases. The worst scenario is 4-R, in which the water content gradually rises from 15% to 55 % over 1200 days because of the wall's over-saturation during the winter and the incapacity to dry out during the cold subarctic summer. The problem is caused by the air layer on the exterior side of the wall. This type of wall has difficulties rejecting all the absorbed moisture because of the stocked humidity in the air layer. An oscillation movement, which may be explained by moisture adsorption-desorption over the winter, and summer periods, accompanies this increasing tendency. The TWC increases from 15 % to 20 % during the first oscillation in 4-R, then drops to 17 % during the summer period, and progressively climbs to 55 % after three winter-summer cycles. In 4-B, the TWC decreases progressively (with winter-summer oscillations) from 18 % to 8 % which means that the wall is drying out during summer. Cases 3-B and 3-R, on the other hand, show quasi-periodic graphs which mean the dynamic equilibrium is reached due to the higher thickness of straw about 440 mm. The cited walls show

similar oscillations during each winter-summer phase (for Brasilia-Brazil, the first winter period is situated between the 200th and the 400th day of simulation), but the maximum TWC remains different due to the different weather conditions. The maximum value in case 5-B is about 20 %, before starting to decrease as the construction is drying out. The minimal value in summer for the same case is about 15 % and during the next years, the dynamic equilibrium is reached. This behavior is explained by the presence of layers such as wood wool, which has low vapor permeability.

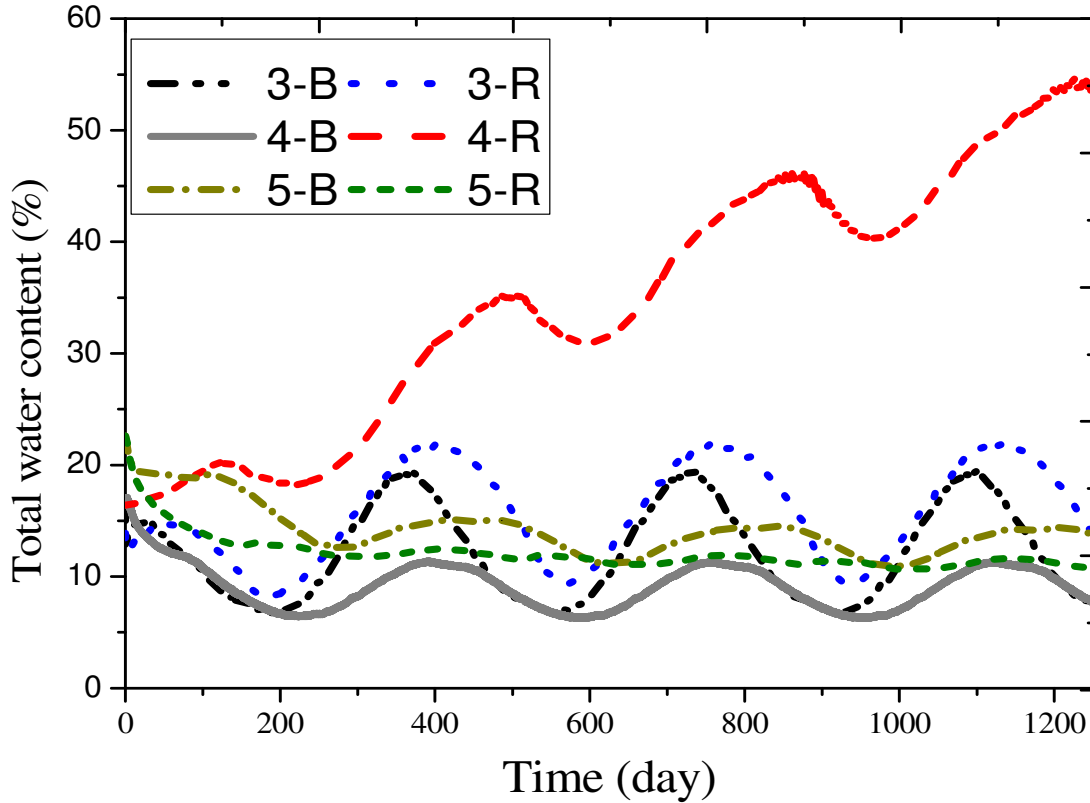


Figure 10: The day-averaged total water content variation for cases three, four, and five over four years under R- the Arkhangelsk-Russia weather and B- the Brasilia-Brazil weather

On the other hand, the WC variation of case 5-R does not match with the previous cases since the curve is flat and there are no oscillations. The TWC keeps decreasing from about 20 % to 10 % during four years. This behavior is mainly due to the high water vapor diffusion resistance factor of the hardwood layer covering both sides of the straw layer, thus reducing moisture transfer to and from the straw. Therefore, the current criterion shows that all the walls can dry out except in some cases in specific weather. The problem was noticed in the first, second, and fourth cases for Arkhangelsk-Russia. This can be related to the subarctic Russian weather, which is characterized by a very cold winter with temperatures that reach $-30\text{ }^{\circ}\text{C}$, and RH that reaches 90 %. The increasing trend of the TWC factor may cause moisture problems, which is studied by calculating the dryness rate.

4.2. Dryness rate

The DR rate is the difference between the initial water content (TWC_i) and the final water content (TWC_f) divided by the initial water content over four years as shown in equation (9). **Figure 11** presents the DR for all wall configurations and all the considered climate conditions.

$$DR = \frac{TWC_i - TWC_f}{TWC_i} \times 100 \quad (9)$$

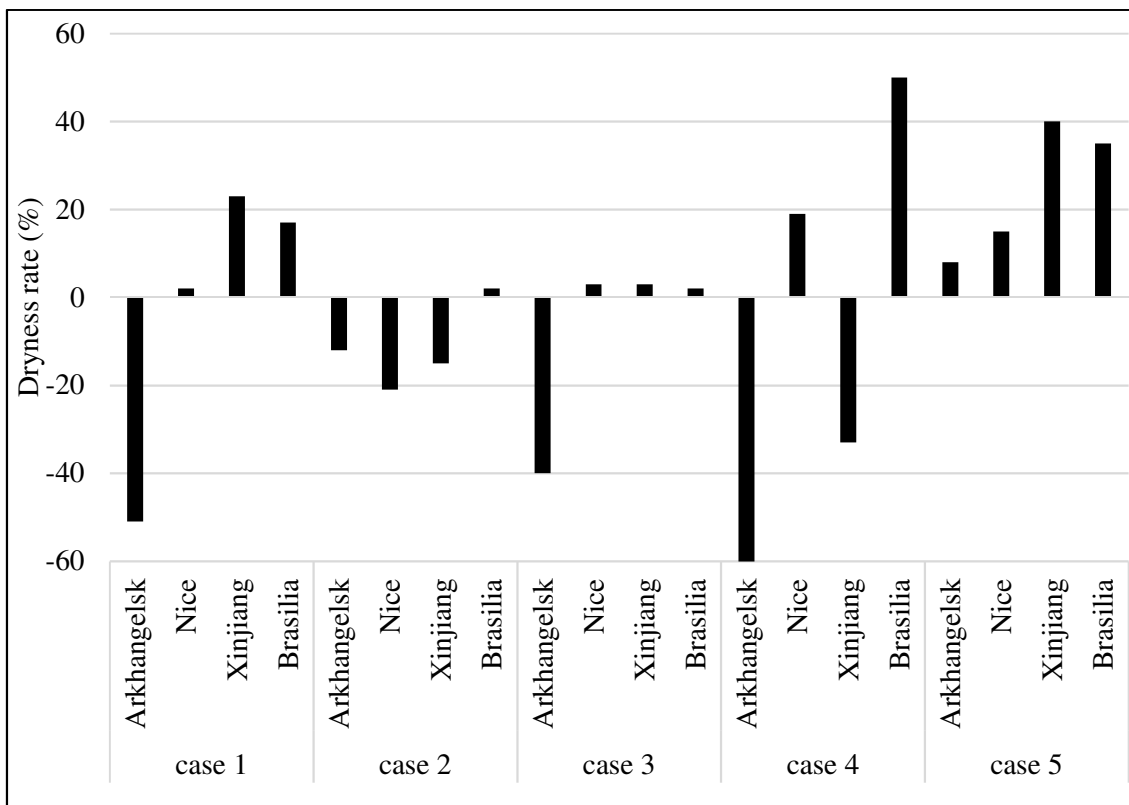


Figure 11: The dryness rate of all cases in all climate conditions for four years

Negative rates mean that the wall is absorbing the humidity and the moisture over the years while positive rates mean that the wall rejects progressively the humidity during the studied period. Not surprisingly, for all weather conditions in case 5, the rates are positive. This type of configuration provides high thermal insulation, which helps to raise the average temperature in the wall, and therefore delays saturation. It should be noted that the temperature controls the water vapor movement by limiting the maximum saturation water vapor pressure. If the saturation pressure is low (in cold weather) then the drying rate will decrease because of the low difference between the saturation pressure and the water vapor pressure. Case 4 has a higher DR than case 5 for the tropical Brazilian weather condition due to the influence of the outer air gap in hot climates. In case 4 for the subarctic continental Russian weather condition, the lowest DR is likewise found due to the influence of the outer air gap in cold climates. It can be seen that the air gap is beneficial in hot climates cases and is a drawback in cold climates cases. The third wall, which is made of a 440 mm straw layer, has a negative DR for the subarctic continental Russian weather (-40 %) and roughly 3 % for all other weathers. It can be explained by the porous nature of the straw, which allows humidity to pass through until its saturation in cold weather. The different results between case 1 and case 2 are due to the higher water diffusion resistance factor and thickness for the hardwood layer.

Therefore, the type of the covering materials and their thickness explain the obtained results since the exterior insulation material improves the dryness of the wall, by the indoor conditions, and by the outdoor weather [15]. In addition, the damaging effect of mold growth and moisture presence can be reduced by minimizing the condensation risk (CR) of the surfaces.

4.3. Condensation risk

Figure 12 indicates the percentage of time when the CR occurs in the considered walls. Results show that the maximum risk of surface condensation, about 60 %, occurs in all structures for the Russian weather and that the minimum CR, about 0 % to 5 %, occurs in all cases for the tropical Brazilian weather. The CR is explained by the direct contact of the wall with the cold environment that leads to low indoor surface temperatures, or by the high RH in the wall. This fact is clear since Arkhangelsk-Russia has a maximum outdoor temperature and RH of about 30 °C and 100 % respectively, and a minimum outdoor temperature and RH of about -30 °C and 23 %, while Brasilia-Brazil has a maximum temperature and RH of about 32 °C and 90 % and a minimum temperature and RH of about 11 °C and 20 %. In addition, the exterior insulation in the building envelope affects the CR as the lowest values are obtained for case 5 for all climates. The layers of wood wool, hardwood, cement plaster, and air gap contribute to the wall's thermal insulation. These layers assist in raising the temperature of the interior layers and surfaces above the dew point temperature of the room to prevent the condensation risk, especially during the winter.

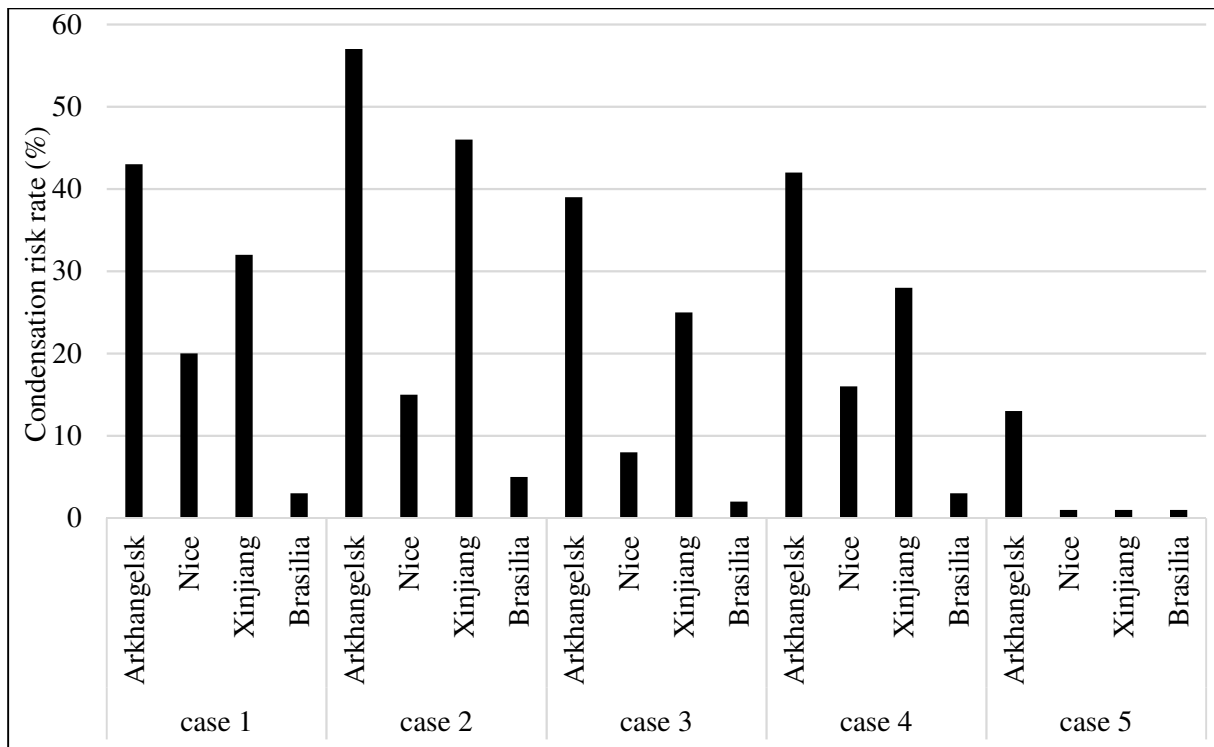


Figure 12: The time percentage where the condensation might occur for all cases over four years

4.4. Mold growth

The decisive parameters for mold growth are humidity and temperature. WUFI generates the isopleth graphs that show the hygrothermal condition of a wall based on its humidity and temperature. As an example, **Figure 13** compares the isopleth graphs of the last two cases under the subarctic continental Russian climate conditions (4-R and 5-R). Both cases correspond to minimal dryness rates as shown in **Figure 11**. In case 4, the hygrothermal conditions at the interior surface cross both Lim 1 and Lim 2 curves while in case 5, they stay below the curves. Consequently, mold growth problems will occur in case 4. For the other cases, results show a risk of mold growth only for the first case under the subarctic continental Russian climate conditions.

Furthermore, a risk of composting can occur when the moisture levels are high at not too low temperatures. Among all simulated cases, the first and fourth cases present a risk of composting of the straw layer in the Russian weather only. The temperature and average RH of the straw layer respectively reach 15°C and 85% for case 1 and 20°C and 90% for case 4 (see **Figure 13**).

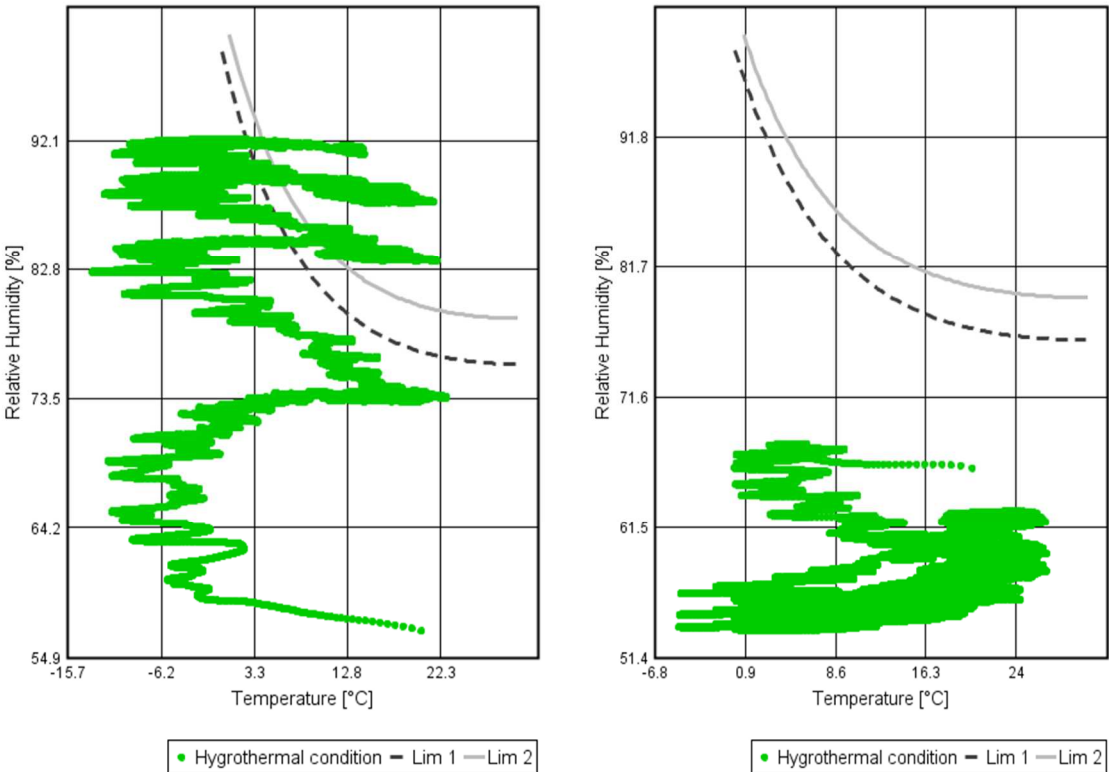


Figure 13: The isopleth for case 4 (left) and case 5 (right) tested with Arkhangelsk-Russia climate condition

4.5. ASHRAE criterion

Table 6 summarizes the results on the ASHRAE criteria once applied to the selected cases. It was observed that the ASH criterion is not respected 30 %, 17 %, 28 %, 73 %, and 2 % of the time respectively in cases one, two, three, four, and five for Arkhangelsk-Russia where the RH surpasses the 80 % limit and reaches 85 % after four years. The high risk in the subarctic continental Russian weather only, in all cases, is explained by the exterior and interior conditions that affect the humidity of exterior and interior layers. In that climate, the first four wall configurations are not able to dry out, as seen in Figure 11. For the same reasons as explained for the DR criterion, these walls have high relative humidity. The variation of the average RH inside the wall in case 3-R over 100 days is presented in **Figure 14**. The thickness of the straw layer plays an important role in regulating the humidity of the whole structure. The RH decreases from 80 % to 30 %. The air and the hardwood layers also participate in moderating the humidity fluctuations by preventing the indoor air humidity to penetrate the wall.

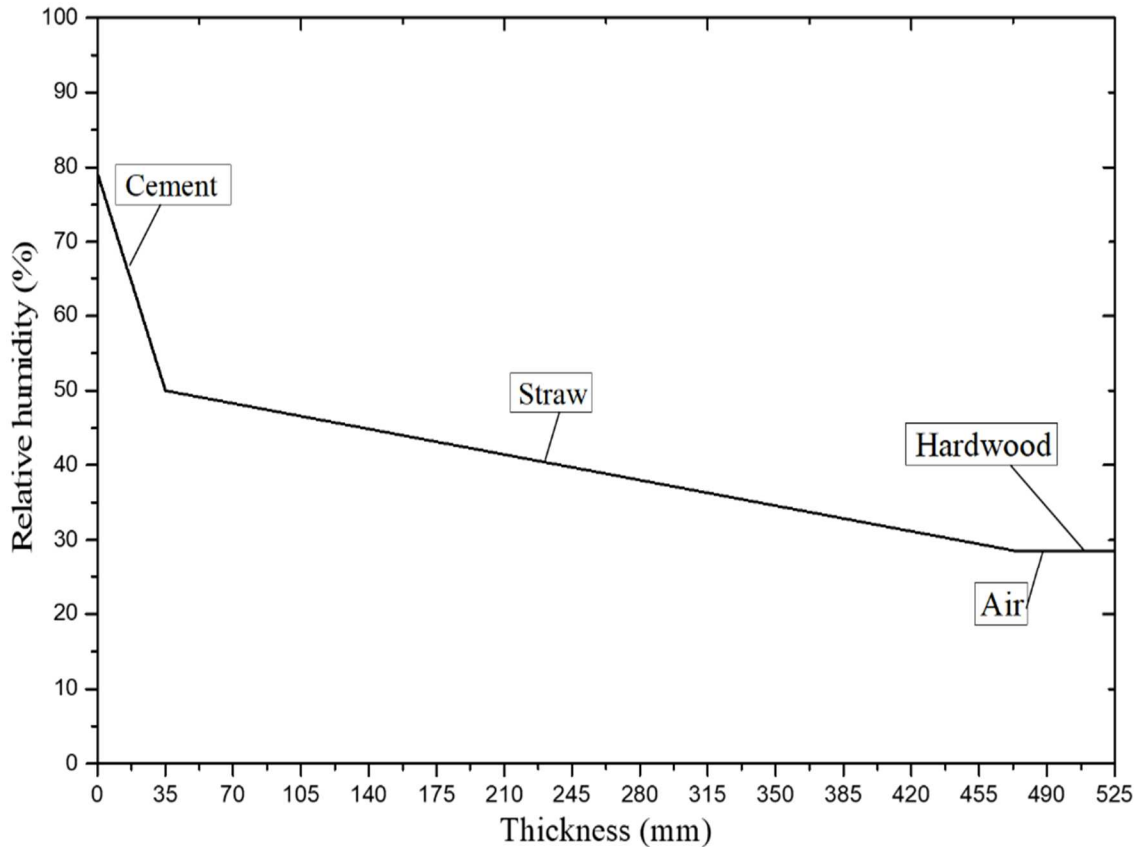


Figure 14: The relative humidity distribution inside the wall (3-R) through all the layers during 100 days in winter

Table 6: Computed results from the straw walls cases regarding the ASHRAE standard (ASH)

ASH criterion	Case 1	Case 2	Case 3	Case 4	Case 5
Arkhangelsk -Russia	Risk (30 %)	Risk (17 %)	Risk (28 %)	Risk (73 %)	Risk (2 %)
Nice-France	No risk	No risk	Risk (2 %)	No risk	No risk
Xinjiang-China	No risk	No risk	No risk	No risk	No risk
Brasilia-Brazil	No risk	No risk	No risk	No risk	No risk

4.6. Time lag and decrement factor

Those two important parameters of wall thermal inertia are calculated based on equations (3) and (4) for all of the wall configurations. It is known that the material's thermal diffusivity and thickness especially affect the time lag and the decrement factor. To obtain a low decrement factor and high time lag, the thermal diffusivity of a wall should be decreased by reducing the thermal diffusivity of its layers, while the wall thickness should be increased. Results in **Table 7** show that the first and the second wall have the same time lag but different decrement factors. The second wall has a higher decrement factor because the hardwood has a higher thermal diffusivity than the cement layer. In addition, the third case shows better values than the fourth case due to the straw layer thickness that provides lower thermal diffusivity. The different layers

used in the last case, such as wood wool, hardwood, and cement layer, reinforce the thermal mass of the wall. Therefore, the fifth case obtains the highest time lag of about 8 hours and 30 minutes and the lowest decrement factor of value 0.05.

Table 7: Computed results from the straw walls cases regarding time lag and decrement factor

	Case 1	Case 2	Case 3	Case 4	Case 5
$\phi(h)$	6h30	6h30	7h30	7h	8h30
$f(-)$	0.06	0.07	0.055	0.065	0.05

5. Proposed Solutions

The hygrothermal problems can be solved using several measures such as increasing the straw thickness, adding a vapor retarder layer, adding an unventilated air layer, and controlling the indoor conditions. A higher thickness of straw may have a good effect since it reinforces the wall permeability and its thermal resistance. To confirm this hypothesis a new case (3-R/360) is simulated corresponding to case 3 with a reduced straw thickness of 360 mm. The results are illustrated in **Figure 15**. Whereas the total water content reached a permanent regime in case 3 under the subarctic continental Russian climate (3-R in **Figure 10**), it is increasing consistently for the new 3-R/360 case over 4 years. Besides, high indoor RH has a critical impact on the behavior of straw-based envelopes. For example, case 5-R passed the TWC criterion under the normal indoor conditions (40 %- 60 % RH) (**Figure 10**). However, this behavior changes when increasing the indoor RH to 60 % in winter and 90 % in summer. Under these new indoor conditions, **Figure 15** shows that the WC of case 5-R increases over four years without attaining equilibrium.

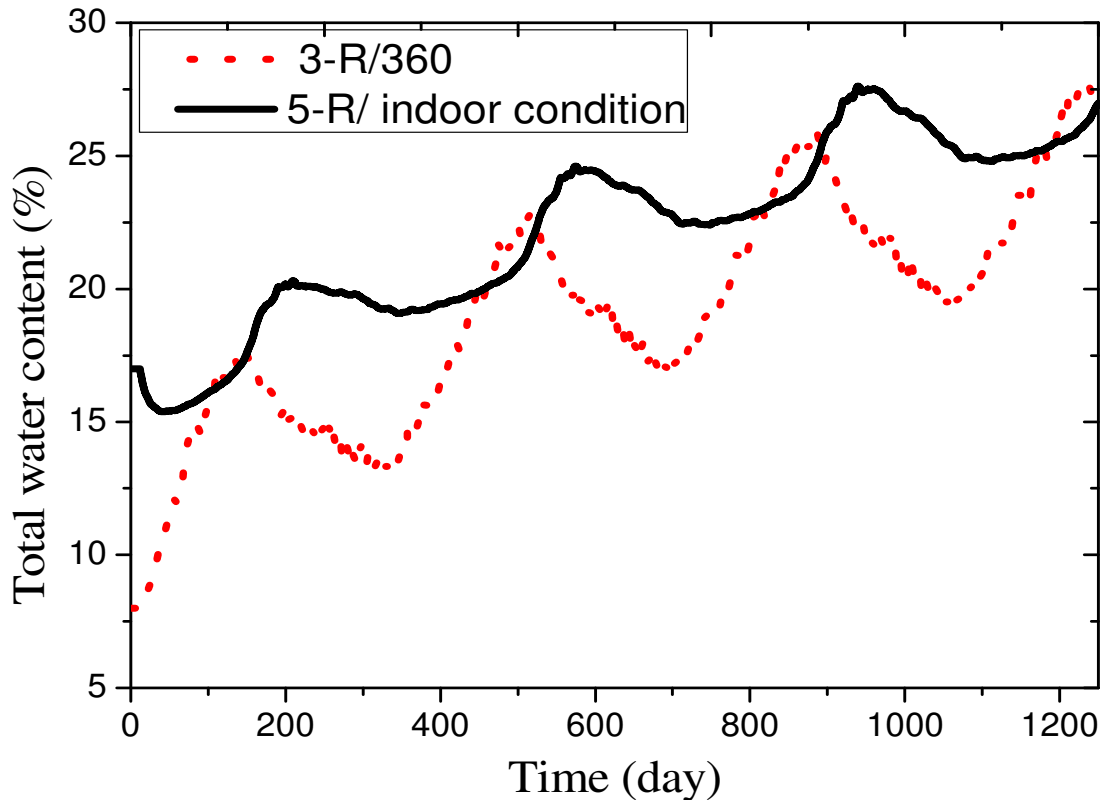


Figure 15: The daily total water content of case 3 (3-R/36) with a straw thickness of about 36 cm and case 5 (5-R) under high indoor relative humidity in Arkhangelsk-Russia for four years

The use of a material that retards the transmission of water vapor is an adequate solution to eliminate the risk of mold growth. For example, by adding a vapor retarder layer behind the interior plaster in 4-R, the dryness rate increases and the hygrothermal conditions stay below the limiting curves as can be seen in **Figure 16**. The same result is reached by increasing the thickness to 440 mm in the 4-R case.

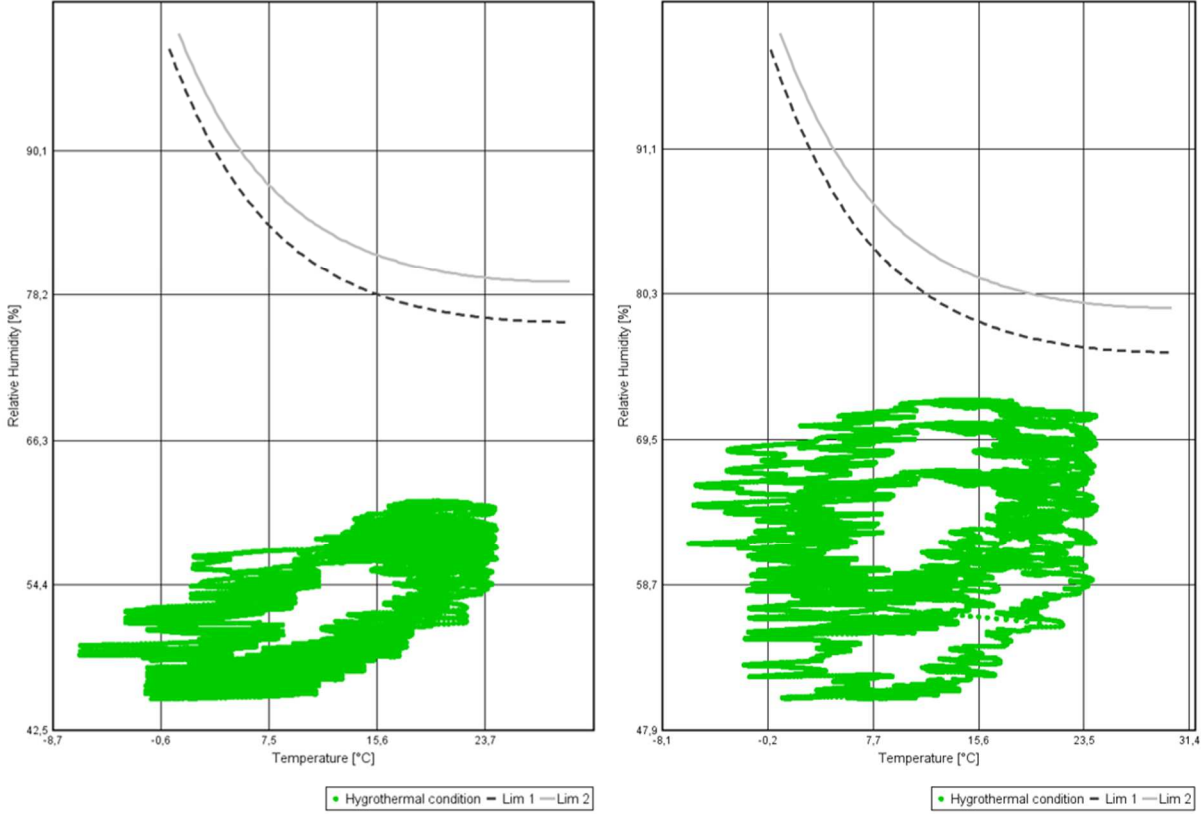


Figure 16: The isopleth for case 4 with vapor retarder layer (left) and with high straw thickness layer (right) tested with Arkhangelsk-Russia climate condition

Composting may be prevented in case 1-R and 4-R by using an exterior ventilated rain screen and a lime layer on both sides of the straw wall. **Figure 17** depicts the impact of these layers through the isopleth of the case 1-R. The maximum RH drops from roughly 90 % (as described in section 4.4) to 54 %. Furthermore, the dryness rate is determined at about -5 %, indicating the wall's capacity to dry. These findings show that the wall's durability related to the condensation and composting risks is improved, especially during the winter. The ventilated rain screen reduces water and humidity infiltration from the outside, while the lime layer enhances the permeability of the wall, which allows for quick drying out.

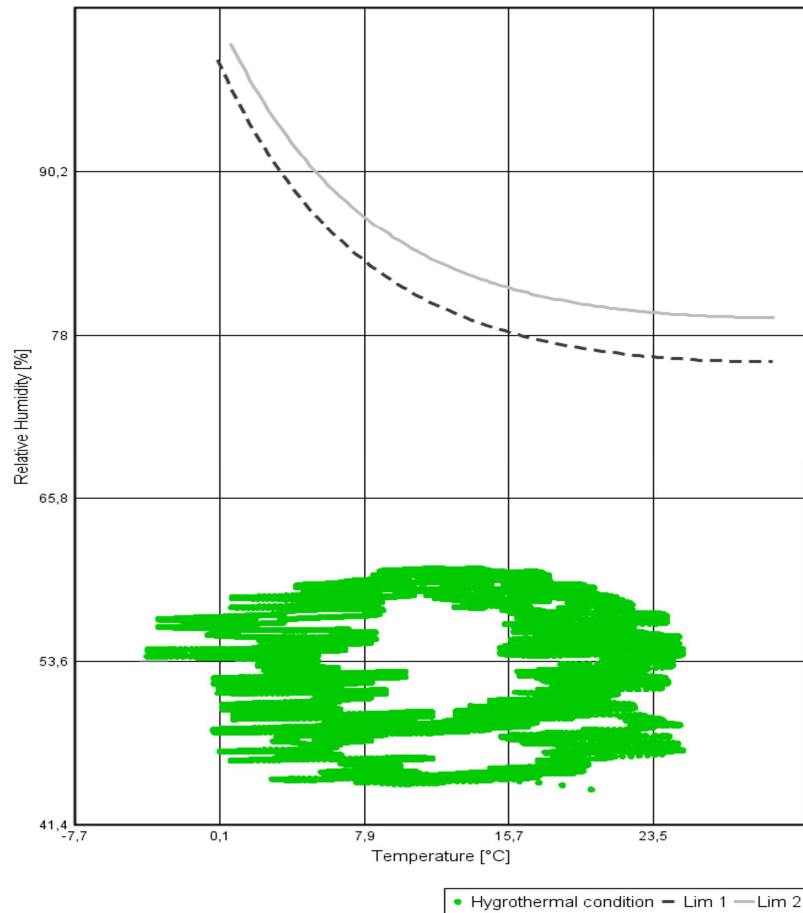


Figure 17: The isopleth for case 1-R with ventilated rain screen and lime layer

The condensation risk and the ASH failure in case 2-R can be avoided by adding an unventilated air layer or an insulating material at the exterior side of the straw layer. The gap between the hardwood and the straw reinforces the exterior insulation and helps to increase the interior surface temperature. In this way, the condensation risk decreases from 60 % (case 2 under Russian climates in **Figure 12**) to 11 %. At the same time, the ASH criterion is respected during the whole period since the risk is reduced from 17 % (case 2 under subarctic continental Russian climates in **Table 6**) to 2 %. It was noticed through these additional simulations that the application of a solution to meet one particular hygrothermal criterion could solve problems on other criteria at the same time.

6. Discussion

Straw construction spreads worldwide regarding its wide economic and environmental advantages. Despite its promising characteristics, it may include moisture and condensation risks leading to health, stability, and durability problems. Interior and exterior humidity, driving rain, ground moisture, and leakage can all generate moisture in the straw walls. For this reason, the current research studies the hygrothermal behavior of various straw wall compositions numerically.

From the obtained results, some problems are detected for all wall configurations under the subarctic continental climate weather of Arkhangelsk, Russia. Such cold and wet climate weather with a high level of air RH are prone to cause serious moisture issues [55]. Cold weather generates low surface temperatures that are close to the dew point temperature, which increases the condensation risk even for moderate indoor RH levels. The difference between

the saturation pressure and the water vapor pressure is also reduced, which leads to condensation risks within the wall. This can explain the high condensation risk of the four first cases, which can reach 80% of the simulated time, particularly for the subarctic continental Russian and cold desert Chinese weather. This problem can be avoided by reinforcing the exterior insulation. The climate condition in Arkhangelsk-Russia also explains the lower dryness rate when compared to the other simulated climates.

The simulated results show that the first and fourth cases present mold growth and composting risks for the subarctic continental climate only. Both DR and MG problems can be avoided by adding a vapor retarder layer or by increasing the straw thickness. The composting risk can be prevented by adding an exterior ventilated rain screen and a lime layer on both sides of the straw wall. In the third case under all the climates except Arkhangelsk-Russia, the total water content is stable and the RH is lower than 80 % over four years, thanks to the air layer in the interior side and the high thickness of the straw. These results are different for 3-R because of the interior insulation and the low interior surface temperature. The interior layers in 4-R, 4-C, 3-C, and 5-R led the interior surface temperature to go low reducing the drying capability of the building envelope. The thermal inertia was assessed by comparing the time lag and the decrement factor, associated with the heat storage capacity of each wall. The time lag of the first two cases was 6 hours and 30 minutes while for cases three and four, it was 7 hours. The last case having in its structure multiple wood layers, wood wool layer, and straw layer, had the highest time lag of about 8 hours and 30 minutes. All cases show a low decrement factor varying between 0.05 and 0.07. Such results show that walls with the highest thickness and lowest thermal diffusivity feature higher time lags and lower decrement factors.

This study aimed to associate to each climate the optimum wall composition from a hygric and thermal point of view. It was noticed that hygrothermal issues occurred mainly in the cold or/and the humid weather. The first, second and fourth wall configurations have similar behavior and can be used in temperate-Mediterranean (Csa) and savanna (Aw) climates such as Nice and Brazilia. The third case shows good thermal properties and can be used in cold desert climates (BWk) such as Xinjiang. The last case did not present hygrothermal problem and mold growth in all climates with normal indoor conditions and can be used in all climates, including the subarctic continental climates (Dfc) such as Arkhangelsk. The presence of the wood wool as exterior insulation and the interior air layer in case five prevented hygric issues. For this reason, it has better performance under all conditions.

7. Conclusion and future work

Straw bales are increasingly used as construction material for ecological and economic reasons. They have high insulation performance and are easily applied. The hygroscopic properties of the straw influence the performance of the wall and may lead to its degradation. This study assesses the hygrothermal behavior of different multilayer straw walls under different boundary conditions. Accordingly, a model was developed using WUFI software to solve the coupled heat and moisture transfer within the wall. The model was validated using experimental results from the literature. Next, numerical tests considered five straw wall structures under four weather conditions to assess the temperature and RH variation inside the wall. The chosen hygrothermal evaluation criteria were the total water content, the drying rate, the condensation risk, the mold growth, the moisture quantity, the time lag, and the decrement factor. Results show that:

- 360 mm straw walls covered by a 20 mm cement layer on both sides are suitable for Mediterranean (Csa) and savanna (Aw) climates. This type of wall has:
 - Time lag and decrement factor of 6h30 and 0.06, respectively.

- Mold growth problems with dryness and condensation risk rates about -50 % and 43 %, respectively, under the subarctic continental Russian weather.
- 360 mm straw walls covered by 30 mm hardwood boards on both sides are suitable for Mediterranean (Csa) and savanna (Aw) climates. This type of wall has:
 - Dryness rates of -12 %, -21 %, -15 %, under the subarctic continental Russian, the Mediterranean French, and the cold desert Chinese climates, respectively.
 - A high condensation risk of 57 % under subarctic continental Russian weather.
 - Time lag and decrement factor of 6h30 and 0.07, respectively.
- The third wall composed of a 35 mm exterior cement layer, 440 mm straw layer, 30 mm interior unventilated air gap, and 15 mm hardwood layer is suitable for cold desert climates. This type of wall has:
 - Time lag and decrement factor of 7h30 and 0.055, respectively.
 - Dryness and condensation risk rates about -40 % and 39 %, respectively, under the continental Russian weather.
- The fourth wall composed of a 40 mm exterior hard-wood layer, 30 mm unventilated air gap, 20 mm exterior cement plaster, 360 mm straw layer, and 20 mm interior cement plaster is suitable for Mediterranean (Csa) and savanna (Aw) climates. This type of wall has:
 - Time lag and decrement factor of 7h and 0.065, respectively.
 - Mold growth issues and lowest dryness rate of -60 % under the subarctic continental Russian weather.
- Walls was composed of 10 mm exterior cement plaster, 40 mm wood wool layer, 18 mm hard-wood board, 360 mm straw layer, 10 mm hard-wood board, 50 mm unventilated air gap, 30 mm hard-wood board, and 15 mm interior cement plaster are suitable for all climates including the subarctic continental climate. This type of walls:
 - Have time lag and decrement factor of 8h30 and 0.05, respectively.
 - Respect the ASHRAE criterion in all climates except the subarctic continental Russian weather 2 % of the time.
 - Have dryness and condensation risk rates of 10 % and 12 %, respectively, under the subarctic continental Russian weather.
 - The wood wool and hardwood layers help the fifth wall to dry out and decrease the condensation risk.
- The air gap is beneficial in hot climates and has a negative impact in cold climates.

A full study should be done to examine the driving rain effect on the hygrothermal property of the five chosen straw walls. In addition, these walls should be compared from an energetic and ecological point of view by calculating the heating and cooling loads of the whole building under different climate conditions. Such a study will lead to a compromise between the hygrothermal performance of the envelope and the energetic performance of the building to associate the ideal wall structure with the appropriate climate.

Acknowledgments

This research was carried out within the ECOMAT project funded by the 2015-2021 French state-region development plan contract (CPER).

References

- [1] E. Vaughan, Straw-Bale Construction: Harvesting Its Potential as an Affordable and Energy-Efficient Building Strategy | Briefing | EESI, Environmental and Energy Study Institute. (2008). <https://www.eesi.org/briefings/view/straw-bale-construction-harvesting-its-potential-as-an-affordable-and-energ>.
- [2] M. Bouasker, N. Belayachi, D. Hoxha, M. Al-Mukhtar, Physical Characterization of Natural Straw Fibers as Aggregates for Construction Materials Applications, *Materials*. 7 (2014) 3034–3048. <https://doi.org/10.3390/ma7043034>.
- [3] I. Pešenjanski, B. Miljković, M. Vićević, Pyrolysis Kinetic Modelling of Wheat Straw from the Pannonian Region, *Journal of Combustion*. 2016 (2016). <https://doi.org/10.1155/2016/9534063>.
- [4] L. Zhang, K. Chen, L. He, L. Peng, Reinforcement of the bio-gas conversion from pyrolysis of wheat straw by hot caustic pre-extraction, *Biotechnology for Biofuels*. 11 (2018) 72. <https://doi.org/10.1186/s13068-018-1072-5>.
- [5] USDA ERS - Home, (n.d.). <https://www.ers.usda.gov/>.
- [6] A. Shea, K. Wall, P. Walker, Evaluation of the thermal performance of an innovative prefabricated natural plant fibre building system, *Building Services Engineering Research and Technology*. 34 (2013) 369–380. <https://doi.org/10.1177/0143624412450023>.
- [7] J. Vejelienė, Processed straw as effective thermal insulation for building envelope constructions, *Engineering Structures and Technologies*. 4 (2012) 96–103. <https://journals.vgtu.lt/index.php/EST/article/view/4715/4037>.
- [8] S. Džidić, Fire Resistance of the Straw Bale Walls, *Zbornik Radova Građevinskog Fakulteta*. 33 (2017) 423–432. <https://doi.org/10.14415/konferencijagfs2017.044>.
- [9] A. Trabelsi, Z. Kammoun, Experimental evaluation of acoustic characteristics of straw walls, *Canadian Acoustics*. 46 (2018) 49–57.
- [10] S. Cascone, G. Evola, A. Gagliano, G. Sciuto, C.B. Parisi, Laboratory and in-situ measurements for thermal and acoustic performance of straw bales, *Sustainability*. 11 (2019). <https://doi.org/10.3390/su11205592>.
- [11] A.D. González, Energy and carbon embodied in straw and clay wall blocks produced locally in the Andean Patagonia, *Energy and Buildings*. 70 (2014) 15–22. <https://doi.org/10.1016/j.enbuild.2013.11.003>.
- [12] G. Mutani, C. Azzolino, M. Macr, S. Mancuso, Straw Buildings : A Good Compromise between Environmental Sustainability and Energy-Economic Savings, *Applied Sciences*. 10 (2020). <https://doi.org/10.3390/app10082858>.
- [13] C. Atkinson, Energy Assessment of a Straw Bale Building, 2008. <https://fr.scribd.com/document/258350643/19-Energy-Assessment-of-a-Straw-Bale-Building-1>.
- [14] J. Wihan, Humidity in straw bale walls and its effect on the decomposition of straw, 2007. https://www.enertech.fr/pdf/45/humidite_murs_paille.pdf.
- [15] M. Ibrahim, E. Wurtz, P.H. Biwole, P. Achard, H. Sallee, Hygrothermal performance of exterior walls covered with aerogel-based insulating rendering, *Energy and Buildings*. 84 (2014) 241–251. <https://doi.org/10.1016/j.enbuild.2014.07.039>.

- [16] T. Ashour, H. Georg, W. Wu, Performance of straw bale wall: A case of study, *Energy and Buildings*. 43 (2011) 1960–1967. <https://doi.org/10.1016/j.enbuild.2011.04.001>.
- [17] O. Douzane, G. Promis, J.M. Roucoult, A.D. Tran Le, T. Langlet, Hygrothermal performance of a straw bale building: In situ and laboratory investigations, *Journal of Building Engineering*. 8 (2016) 91–98. <https://doi.org/10.1016/j.job.2016.10.002>.
- [18] R. Fauconnier, L'action de l'humidité de l'air sur la santé dans les bâtiments tertiaires , *Chauffage Ventilation Conditionnement*. (1992) 57–62.
- [19] M. Lawrence, A. Heath, P. Walker, Determining moisture levels in straw bale construction, *Construction and Building Materials*. 23 (2009) 2763–2768. <https://doi.org/10.1016/j.conbuildmat.2009.03.011>.
- [20] K. Strømdahl, *Water Sorption in Wood and Plant Fibres*, Denmark, 2017. orbit.dtu.dk (accessed September 7, 2020).
- [21] R. Gallegos-Ortega, T. Magaña-Guzmán, J.A. Reyes-López, M.S. Romero-Hernández, Thermal behavior of a straw bale building from data obtained in situ. A case in Northwestern México, *Building and Environment*. 124 (2017) 336–341. <https://doi.org/10.1016/j.buildenv.2017.08.015>.
- [22] Utilisation de la paille en parois de maisons individuelles a ossature bois, (2004). <https://docplayer.fr/60439589-Utilisation-de-la-paille-en-parois-de-maisons-individuelles-a-ossature-bois.html>.
- [23] C. Rye, C. Scott, The spab research report 1. U-value report, 2012. www.spab.org.uk.
- [24] T. Ashour, The use of renewable agricultural by-products as building materials, 2003. <https://doi.org/10.13140/RG.2.1.2887.7285>.
- [25] K.A. Sabapathy, S. Gedupudi, Straw bale based constructions: Measurement of effective thermal transport properties, *Construction and Building Materials*. 198 (2019) 182–194. <https://doi.org/10.1016/j.conbuildmat.2018.11.256>.
- [26] A. Chaussinand, J.L. Scartezzini, V. Nik, Straw bale: A waste from agriculture, a new construction material for sustainable buildings, *Energy Procedia*. 78 (2015) 297–302. <https://doi.org/10.1016/j.egypro.2015.11.646>.
- [27] WUFI, (n.d.). <https://wufi.de/en/>.
- [28] H. Künzel, *Simultaneous Heat and Moisture Transport in Building Components One- and two-dimensional calculation using simple parameters*, 1995.
- [29] H. Künzel, A. Holm, *WUFI-2D Program description*, Holzkirchen, 2000.
- [30] A. Mesa, A. Arengi, Hygrothermal behaviour of straw bale walls: experimental tests and numerical analyses, *Sustainable Buildings*. 4 (2019) 10. <https://doi.org/10.1051/sbuild/2019003>.
- [31] T. Kalamees, J. Vinha, Hygrothermal calculations and laboratory tests on timber-framed wall structures, *Building and Environment*. 38 (2003) 689–697. [https://doi.org/10.1016/S0360-1323\(02\)00207-X](https://doi.org/10.1016/S0360-1323(02)00207-X).
- [32] M. Kotteck, J. Grieser, C. Beck, B. Rudolf, F. Rubel, World map of the Köppen-Geiger climate classification updated, *Meteorologische Zeitschrift*. 15 (2006) 259–263. <https://doi.org/10.1127/0941-2948/2006/0130>.

- [33] X. Yin, M. Lawrence, D. Maskell, M. Ansell, Comparative micro-structure and sorption isotherms of rice straw and wheat straw, *Energy and Buildings*. 173 (2018) 11–18. <https://doi.org/10.1016/j.enbuild.2018.04.033>.
- [34] J.-P. Costes, A. Evrard, B. Biot, G. Keutgen, A. Daras, S. Dubois, F. Lebeau, L. Courard, Thermal Conductivity of Straw Bales: Full Size Measurements Considering the Direction of the Heat Flow, *Buildings*. 7 (2017). <https://doi.org/10.3390/buildings7010011>.
- [35] M. Ibrahim, P. Henry, E. Wurtz, P. Achard, A study on the thermal performance of exterior walls covered with a recently patented silica-aerogel-based insulating coating, *Building and Environment*. 81 (2014) 112–122. <https://doi.org/10.1016/j.buildenv.2014.06.017>.
- [36] L. Arnaud, C. la Rosa, F. Sallet, Mechanical behaviour of straw construction following the GREB technique, in: *Non-Conventional Materials and Technologies (NOCMAT)*, ResearchGate, Bath, UK, 2009: pp. 1–8.
- [37] A.A. Aznabaev, A.V. Ovsyannikova, A.O. Povzun, Z.A. Gaevskaya, Assessment of straw construction technologies in terms of thermal efficiency of enclosing structures, *Construction of Unique Buildings and Structures*. 43 (2016) 104–116. www.unistroy.spb.ru.
- [38] The concrete conundrum, *Chemistry World*. (2008) 62–66. www.chemistryworld.org.
- [39] I.A. de La Roche, J. O’Connor, P. Tetu, Wood Products And Sustainable Construction, in: *XII World Forestry Congress*, Quebec city, Canada, 2003. <http://www.fao.org/3/XII/1039-A2.htm>.
- [40] M.H. Ramage, H. Burrige, M. Busse-Wicher, G. Fereday, T. Reynolds, D.U. Shah, G. Wu, L. Yu, P. Fleming, D. Densley-Tingley, J. Allwood, P. Dupree, P.F. Linden, O. Scherman, The wood from the trees: The use of timber in construction, in: *Renewable and Sustainable Energy Reviews*, Elsevier Ltd, 2017: pp. 333–359. <https://doi.org/10.1016/j.rser.2016.09.107>.
- [41] Activ Home : Constructions Ecologiques Et Economiques - Activ Home, (n.d.). <https://www.activ-home.com/fr/>.
- [42] Cereal production (metric tons) by Country, (2019). <https://www.indexmundi.com/facts/indicators/AG.PRD.CREL.MT>.
- [43] Athena, B. Steen, Building a Home Using Straw Bale Construction, *MOTHER EARTH NEWS*. (1996). <https://www.motherearthnews.com/green-homes/straw-bale-construction-zmaz95djzgoe>.
- [44] S. Yevgeny, Building with bales in Belarus, *Ecology and Sustainable Development*. (n.d.). <https://www.inforse.org/europe/iae/mae/building.html>.
- [45] K.R.G. Punhagui, É.F. Campos, J.M.B. González, V.M. John, Prospects for the use of wood in residential construction in Brazil - First results, *Key Engineering Materials*. 517 (2012) 247–260. <https://doi.org/10.4028/www.scientific.net/KEM.517.247>.
- [46] ADRA straw bale housing becomes an eco-friendly solution for post-earthquake China - China | ReliefWeb, ADRA. (2009). <https://reliefweb.int/report/china/adra-straw-bale-housing-becomes-eco-friendly-solution-post-earthquake-china>.
- [47] Straw-Bale Construction Gaining Popularity in France, *France Ecotours*. (n.d.). <https://www.myecostay.eu/en/blog/straw-bale-construction-gaining-popularity/>.

- [48] Weather Data | EnergyPlus, (n.d.). <https://www.energyplus.net/weather>.
- [49] ANSI/ASHRAE (2017) Standard 55: 2017, Thermal Environmental Conditions for Human Occupancy, 2017. www.ashrae.org.
- [50] EN 13779:2004-Ventilation for non-residential buildings-Performance requirements for ventilation and room-conditioning systems, 2004. <https://standards.iteh.ai/catalog/standards/sist/3373541e-9989-4e0b-8fe8-> (accessed January 25, 2022).
- [51] J. Straube, J. Smegal, Building America Special Research Project: High-R Walls Case Study Analysis, 2009.
- [52] A. Tenwolde, ASHRAE Standard 160P __ Criteria for Moisture Control Design Analysis in Buildings, 2008.
- [53] Moisture Control Guidance for Building Design, Construction and Maintenance Indoor Air Quality (IAQ), (2013). www.epa.gov/iaq/moisture (accessed August 21, 2021).
- [54] K. Sedlbauer, Prediction of Mould Growth by Hygrothermal Calculation, THERMAL ENVIRONMENTAL and Building Science. 24 (2002). <https://doi.org/10.1106/109719602024093>.
- [55] N.R. Bronsema, Moisture Movement and Mould Management in Straw Bale Walls for a Cold Climate, 2010. <http://uwspace.uwaterloo.ca/handle/10012/5536>.